

Developing a multi-scale modeling system for resilience assessment of green-grey drainage infrastructures under climate change and sea level rise impact



Justin Joyce ^a, Ni-Bin Chang ^{a,*}, Rahim Harji ^b, Thomas Ruppert ^c, Sanaz Imen ^a

^a Department of Civil, Environmental, and Construction Engineering, University of Central Florida, Orlando, FL, USA

^b Watershed Management Section, Pinellas County Government, Largo, FL, USA

^c Florida Sea Grant College Program, Miami, FL, USA

ARTICLE INFO

Article history:

Received 28 May 2016

Received in revised form

28 November 2016

Accepted 29 November 2016

Available online 6 January 2017

Keywords:

Stormwater management

Drainage infrastructure

Resilience assessment

Climate change

Sea level rise

Watershed model

Coastal sustainability

ABSTRACT

Multi-scale modeling analysis is often required for comprehensive resilience assessment of urban drainage infrastructures to account for global climate change impact and local watershed response. The goal of this study was to develop a multi-scale modeling platform for drainage infrastructure resilience assessment in a coastal watershed. The model employs scale-dependent informatics, including hydro-informatics, climate informatics, and geoinformatics, to support a comprehensive hydrodynamic stormwater and hydrologic model, called the Interconnected Channel and Pond Routing Model. Low Impact Development (LID), deemed as green drainage infrastructure, was adopted and assessed in the Cross Bayou Watershed, Florida. The Cross Bayou Canal is the grey infrastructure, which dissects the watershed and connects both Tampa Bay and Boca Ciega Bay on its northeastern and southwestern ends, respectively. Modeling scenarios are driven by watershed-scale rainfall/runoff, coastal high tide, and global sea level rise, respectively or collectively, to evaluate the green-grey drainage infrastructure system in response to current and future coastal flood hazards predicted for year 2030. The quantitative resilience metrics, such as peak inflow reduction at flood zone, were chosen to reflect storms that pose threats to the watershed, now and in the future year 2030, for climate change scenarios derived by the Statistical Downscaling Model. Results indicate that the effectiveness of LID depends on the rainfall type being considered, such as convective storm versus frontal rain, and sub-daily rainfall patterns, as well as a groundwater table analysis.

© 2016 Elsevier Ltd. All rights reserved.

1. Introduction

Hurricane Katrina in 2005 and Hurricane Sandy in 2012 were the costliest flood events ever in the US. The future impact of such events will be exacerbated by increasing population concentrations in cities, with the [UN-Habitat \(2012\)](#) predicting that more than 70% of the world's population will live in cities by 2050. Furthermore, according to NOAA, about 3.2 Billion people worldwide live and work in a coastal strip just 200 km wide, and a full two-thirds, 4Bn, are within 400 km of a coast ([NOAA, 2016a,b](#)). In May 2015, the Florida legislature passed and the governor signed into law SB 1094 to consider future flood impacts in the Florida Comprehensive Plans, particularly from a coastal management perspective. The law

includes requirements for development and redevelopment efforts to reduce flood risk by considering hazards such as high tide events and sea level rise. Risk in this context can be described as the likelihood of a flood hazard occurring with an associated loss or negative impact, which can be expressed as the product of hazard, vulnerability, and exposure. Hazards can be considered physical manifestations or occurrences of adverse events while exposure relates to elements negatively affected by hazards. Vulnerability can be summarized as the propensity or predisposition to be adversely affected or susceptible to harm, and a lack of capacity to cope and adapt ([IPCC, 2014](#)). Although considering the hazards and exposure posed is important, considering vulnerability and adaptive capacity, which are tied to the concept of resilience, are equally important.

Since [Holling \(1973\)](#) introduced the term “resilience” into the study of ecosystems, resiliency-related research has been

* Corresponding author.

exponentially increasing. The concept of resilience has expanded to different disciplines, including (1) engineering resilience, or the ability of the system to resume normal functionality after shock; (2) social resilience, or capacity of humans to anticipate and plan for the future; (3) ecological resilience, or the speed of return to stability domain; (4) material resilience, or the ability of material to absorb energy when elastically deformed; and (5) psychology resilience, or the ability of an individual to withstand stress and bounce back or recover from traumatic situations (Omer, 2013). However, engineering resilience will be important when discussing drainage infrastructure systems. Resilience, when applied to infrastructure systems, implies the ability of such infrastructure systems (including their interconnected ecosystems and social systems) to absorb disturbance and recover after a disturbance (Omer, 2013). In considering the resilience of networked infrastructure systems, Omer (2013) argued that the resilient response of a system results in reduced vulnerability and greater adaptive capacity or reduced susceptibility and greater ability to continue functionality under adverse conditions.

These concepts of vulnerability and adaptive capacity of a system depend on the level of disturbance. De Bruijn (2004) highlighted that the magnitude of disturbance absorbed by a system depends on its reaction. As such, when applied to a stormwater drainage system, the magnitude of disturbance can be represented as the storm event intensity and duration, with the system reaction as peak outflow. Because a smaller (larger) reaction results in larger (smaller) infiltration and capture, a stormwater drainage system would ideally reduce its reaction (i.e., peak inflow/outflow) via increased infiltration and capture of stormwater by the environment. One example is Low Impact Development (LID), in which planning and structural controls can contribute to resiliency in flood management via adaptive capacity. LID, promoted in recent years as an alternative to traditional stormwater drainage systems, utilizes decentralized multifunctional site designs and incorporates on-site stormwater management practices rather than conventional stormwater management approaches that divert flow toward centralized facilities. At the local scale, the use of LID as an adaptation measure can increase onsite storage of runoff. Onsite storage has additional benefits that increase resiliency, such as reducing and delaying the runoff peak discharge (Roseen et al., 2012). As reported by De Bruijn (2004), quantifying the response of an infrastructure system to disturbances can provide tangible information about the resilience of a system over time under a posed hazard. Birgani et al. (2013) analyzed the physical and technical characteristics of resilience in sustainable urban stormwater management and, in quantifying resilience, argued that capturing the disturbance and the time of recovery were required. In determining the amount of disturbance captured, Birgani et al. (2013) expanded on De Bruijn's (2004) assessment by highlighting that when a system is disturbed, the system reacts. When considering the Birgani et al. (2013) and the De Bruijn (2004) studies, the response of a stormwater drainage system to a disturbance such as a storm event can be determined by peak outflow and/or stage within a cross-sectional area of a drainage pipe. Peak outflow can be obtained from outflow hydrographs at points of interest. An additional metric can be obtained by accounting for the time required for the drainage network to "recover" from a disturbance such as a storm event.

To apply the concepts of drainage infrastructure resilience to a real-world case study of flood assessment, the Cross Bayou Watershed, located within Pinellas County near Tampa Bay in west-central Florida, was chosen as a specific example. The Cross Bayou Watershed has been historically sensitive to flooding from hazards such as runoff from rainfall and high tide events, and over the years, storm events and subsequent flooding have damaged the drainage

infrastructure, particularly undersized conveyance systems found throughout the watershed. Drainage infrastructure is increasingly vulnerable with age and urban development, and therefore its adaptive capacity is also reduced when considering future storm events and future hazards such as sea level rise. With increasing vulnerability and decreasing adaptive capacity of the drainage infrastructure over its design life, communities dependent on this infrastructure will also face increased vulnerability and decreased adaptive capacity.

The goal of this study was to develop a multi-scale modeling platform that would help coastal areas, such as the Cross Bayou Watershed in Pinellas County, Florida, assess drainage infrastructure resilience to coastal flood hazards that pose threats to the watershed, now and in the future year 2030. From this study, several important questions were addressed. First, will increases in flooding stress and episodic disturbances of climate variability and sea-level rise favor regime shifts of traditional storm sewer systems toward choosing more low impact development (LID) controls and flood proofing technologies? Second, how will urban storm sewer infrastructure, LID controls, and/or flood proofing technologies alter the hydrologic response of the watershed during different types of storm events? Last, will these regime shifts toward more LID technologies increase resilience of the drainage infrastructure, and what methods or criteria can be implemented to measure the resilience of the drainage system? Rationale for this framework is based on the need to integrate multiple environmental processes with different spatial and temporal scales and extensive datasets that must be collected, processed, and analyzed for applications in the nexus of climate informatics, urban hydroinformatics, and geoinformatics. As such, a comprehensive framework, such as integrated environmental modeling, is needed to account for appropriate environmental processes and their associated information to process and apply toward informing decisions and policies related to the environment (Laniak et al., 2013). From this framework, we hypothesize that a regime shift toward incorporating LID alternatives will be required. In addition, LID implementation within the watershed will alter the hydrologic response of existing drainage infrastructure because LID deployment offers increased resilience via peak outflow reduction over various storm events.

2. Study area

The Cross Bayou Watershed of Pinellas County (Fig. 1), Florida, was selected as a case study because of its vulnerability to coastal flooding and Pinellas County's efforts to implement improved stormwater management to increase the area's adaptive capacity to future hazards. The Cross Bayou watershed encompasses approximately 31 km² (7697 acres), primarily comprising high-density residential, industrial, and commercial areas.

An important feature of the watershed is a 16.9 km (10.5-mile) long constructed tidal canal, the Cross Bayou Canal (Fig. 1), which dissects the watershed and connects both Tampa Bay and Boca Ciega Bay on its northeastern and southwestern ends, respectively. The Cross Bayou Canal also intersects the Pinebrook Canal to the southwest (Fig. 1). Water within the canal can flow in either direction, depending on tidal conditions. This feature, while useful for overall watershed drainage, is potentially hazardous to surrounding communities such as the Mariners Cove residential community (Fig. 2) during high tide events, particularly considering the ongoing threat of sea level rise (NOAA, 2016a,b) near the Tampa Bay region.

Some areas in the watershed are consistently more vulnerable and have a decreased adaptive capacity to flooding. The High Point and Mariners Cove residential communities (Fig. 2) are known for

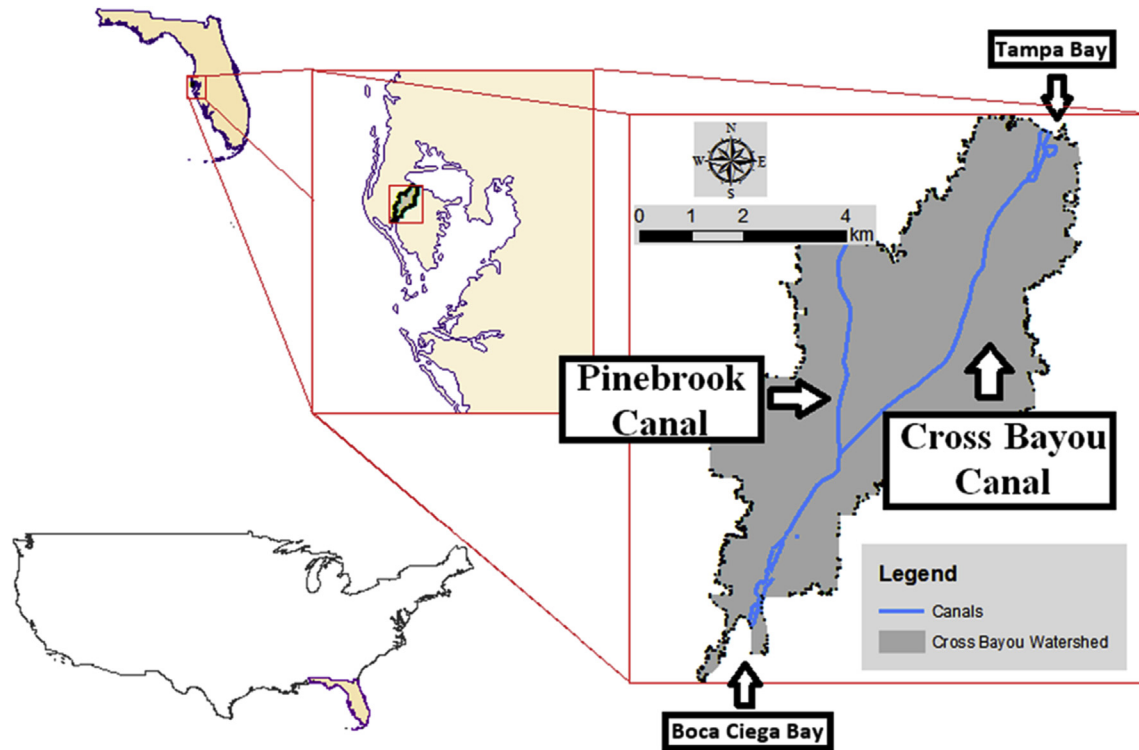


Fig. 1. Extent of Cross Bayou Watershed.

significant flooding from storm events. Flooding in the Mariners Cove community is primarily caused by heavy rains and overflow of the adjacent Cross Bayou canal. Both communities have documented inadequate or inefficient drainage infrastructure due to the age and size of existing drainage systems, which cannot handle runoff from increasing urban development. The Mariners Cove community, in particular, is much closer to the Cross Bayou canal. Areas most vulnerable to hazards also represent those most sociologically vulnerable; both Mariners Cove and High Point communities are predominately low-income areas. The vulnerability and adaptive capacity of these communities are much higher and lower, respectively.

3. Methodology

The methods outlined in this study center around the concept of infrastructure resilience for a coastal urban watershed (Fig. 3) using an informatics-based multi-scale modeling approach. Quantitative resilience metrics were established to quantify engineering infrastructure resilience of the stormwater drainage system within the Cross Bayou watershed under existing and future conditions. To determine the resiliency of the stormwater management system due to flood hazards such as rainfall runoff, high tide, and sea level rise for the future year 2030, a detailed and comprehensive framework is needed, particularly for the complex hydrologic and hydraulic interactions that exist within the Cross Bayou watershed. With the consideration of LID technologies for flood control, this framework contains a multi-scale modeling platform (Fig. 4) that includes a comprehensive hydrodynamic and hydrologic stormwater model, called the Interconnected Channel and Pond Routing Model v.4 (ICPR4) (Streamline Technologies, 2015), in conjunction with informatics methods for effectively presenting resilience-based information and data to stakeholders.

3.1. LID type, sizing, siting & design criteria

Determining sizing and siting options of LID within the watershed depends on not only characteristics such as elevation, slope, soil type, and land cover, but also the existing drainage network and areas of high runoff potential. The existing stormwater drainage network and points of outfall into the Cross Bayou Canal (Fig. 5) can affect vulnerable areas such as Mariners Cove. In this case, the sizing and siting of LID is chosen to (1) reduce runoff collected at major conveyance systems in High Point to offer greater resilience and (2) reduce discharge of runoff into the Cross Bayou Canal from both High Point and adjacent areas surrounding the Pinellas County Jail complex. This is linked to reduce contribution of flooding from runoff and its interaction with high tides within the canal, which could affect downstream communities such as Mariners Cove adjacent to the canal. High Point is characterized by high-density residential areas, institutional areas, and commercial sites, and the area surrounding the Pinellas County Jail complex is characterized by institutional and commercial areas, each with a considerable percentage of imperviousness (some greater than 50%).

The type of LID considered depends on the climate and environmental constraints, if any. The nature of storm events found throughout Florida changes depending on season. During the wet season, between June and October, convective rainfall dominates, whereas during the dry season, between November and May, frontal rain dominates (Ali et al., 2000). Convective rainfall results in many short-duration events with rapidly changing intensity that produce greater peak discharges, whereas frontal rain results in moderate to heavy rainfall over a longer duration that produces greater runoff volume (FHWA, 1984). These differences highlight the need for a range of LID types from swales to detention ponds. With respect to environmental constraints, particularly for the High Point area, space and high groundwater tables are limiting factors.

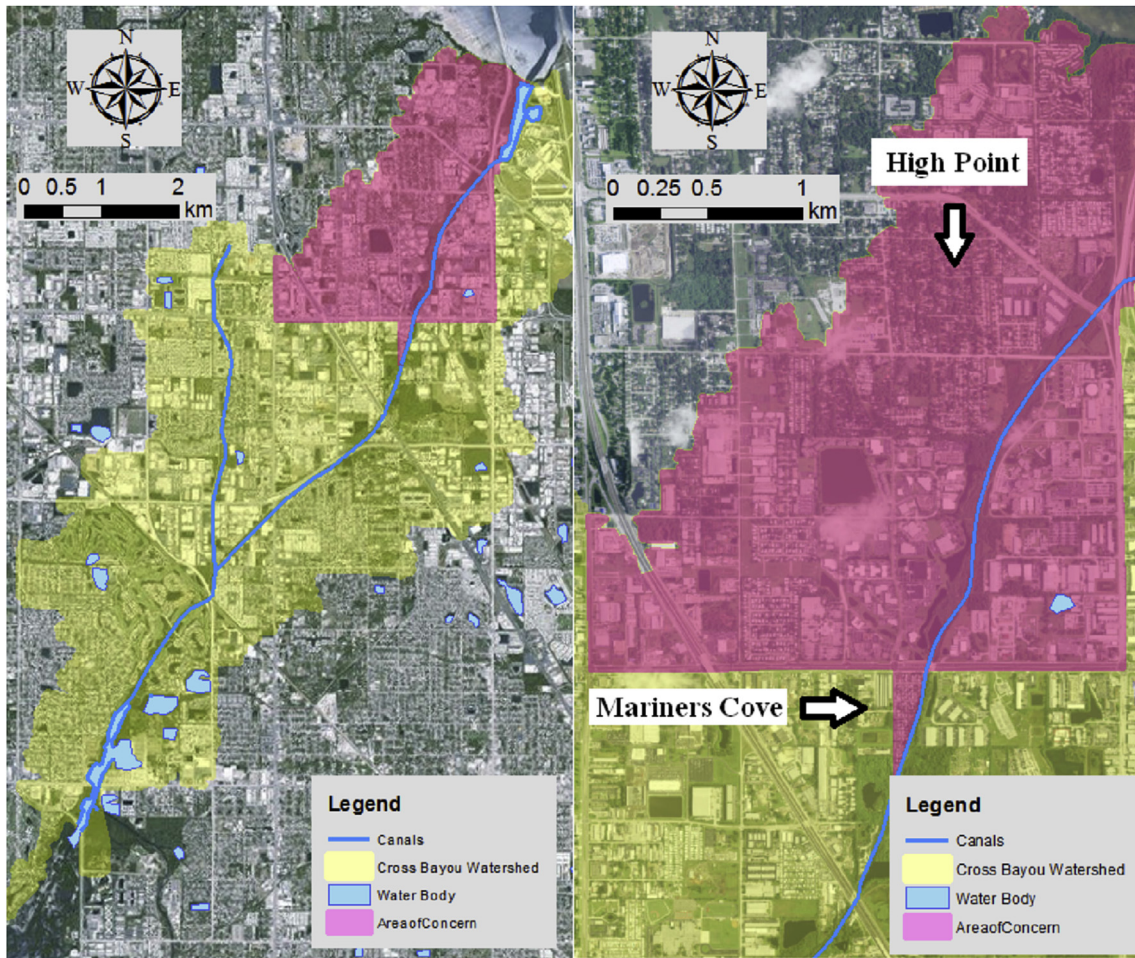


Fig. 2. Area of Concern defines historically vulnerable areas such as the High Point and Mariners Cove residential areas.

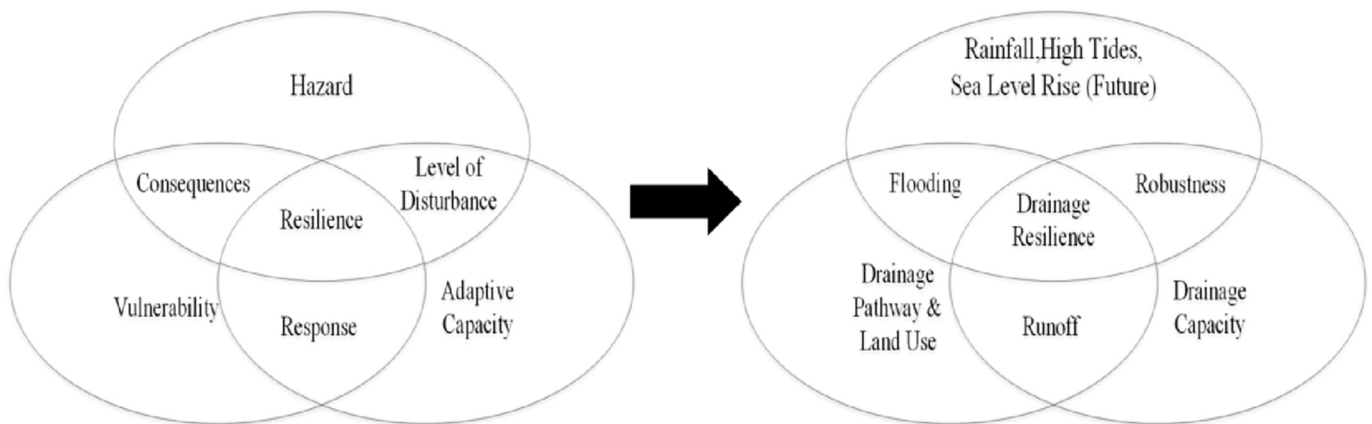


Fig. 3. Methodology framework for drainage resilience.

3.2. LID scenarios

Locations for LID implementation were proposed (Fig. 6), along with LID implementation options (Appendix A) sought for placement at areas within this study. Although the combination of appropriate sizing of LID within these sites near High Points is vast, an important parameter such as percent imperviousness can be useful for determining the appropriate portfolios of LID to be

implemented. Percent imperviousness is a useful parameter in this regard and can be expressed as the total coverage by impervious surfaces to the total land area considered. Percent imperviousness (Table 1) was determined from delineated sub-basins around all major drainage conveyances and existing detention systems (Jones Edmunds and Associates, Inc., 2013).

Several LID scenarios were explored to reduce the percent imperviousness and increase the percent perviousness (i.e.,

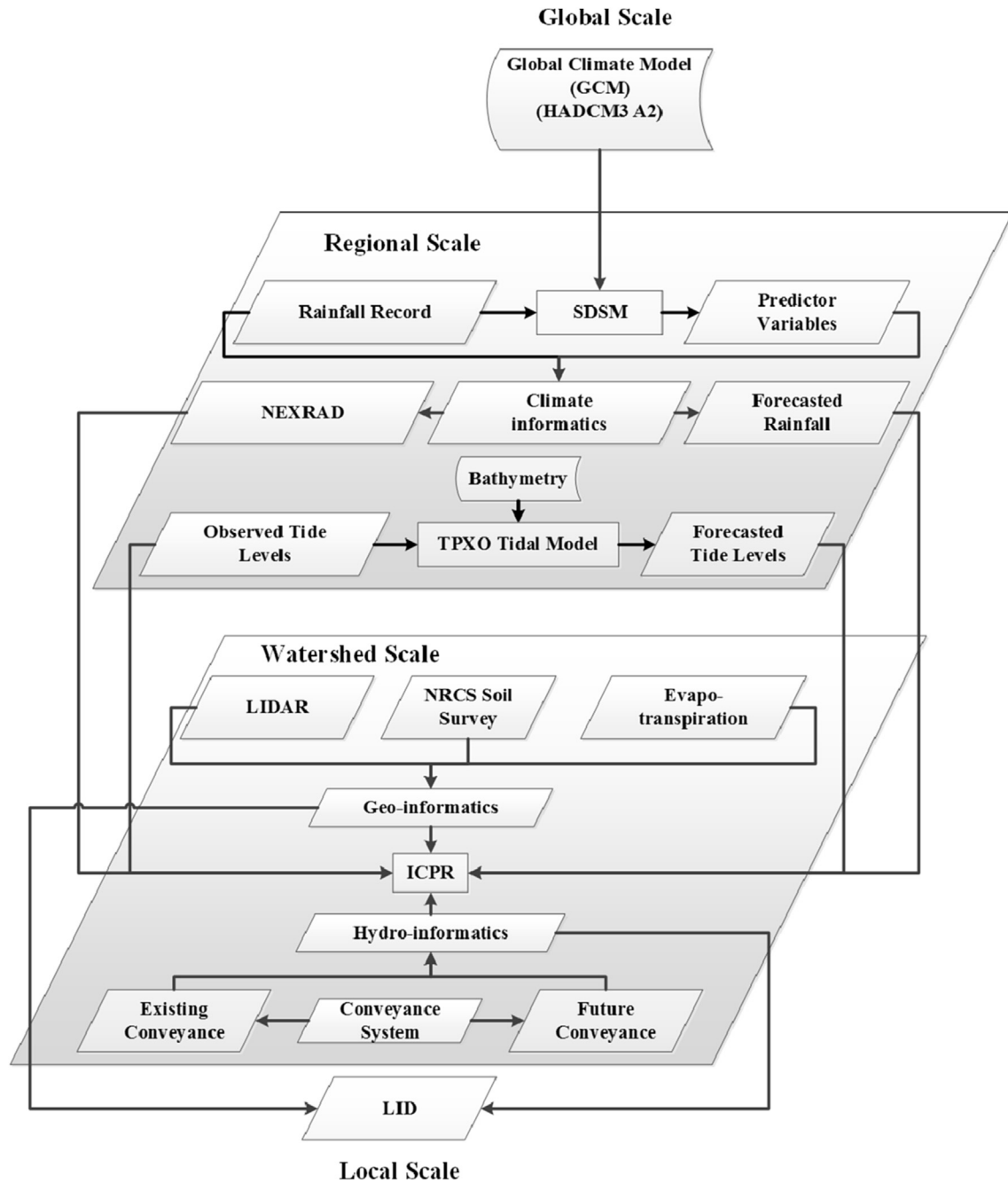


Fig. 4. Data flow diagram highlighting a multi-scale, informatics approach to the modeling framework.

infiltration) (Table 2), assuming that any combination of LIDs for a particular sub-basin has a total area that corresponds with a particular percent pervious. In other words, a 25% impervious reduction in Basin 1 corresponds with a 25% increase in perviousness as a replacement if that particular LID option is implemented. Based on the density of urban space in each sub-basin and soil characteristics, however, the most suitable combination of LIDs can be determined (i.e., Column 5, Table 2).

3.3. Storm scenarios

Design for stormwater management typically relies on a design storm with an associated magnitude or intensity, duration, and

frequency. To reduce flooding potential via incorporation of LID, the likely magnitude, frequency, and duration of rainfall for the Cross Bayou watershed must be determined, typically via statistical techniques based on historic rainfall records such as frequency analysis. Frequency analysis involves relating the magnitude of events to their frequency of occurrence or return period via probability distribution based on the design storm(s) utilized for LID and/or best management practice (BMP) implementation by various agencies across varying levels of governance (national, state, district and county) (Table 3).

Currently, the design, permitting, construction, and operation of stormwater management systems in Florida are governed by laws and regulations of the State of Florida, regional water management

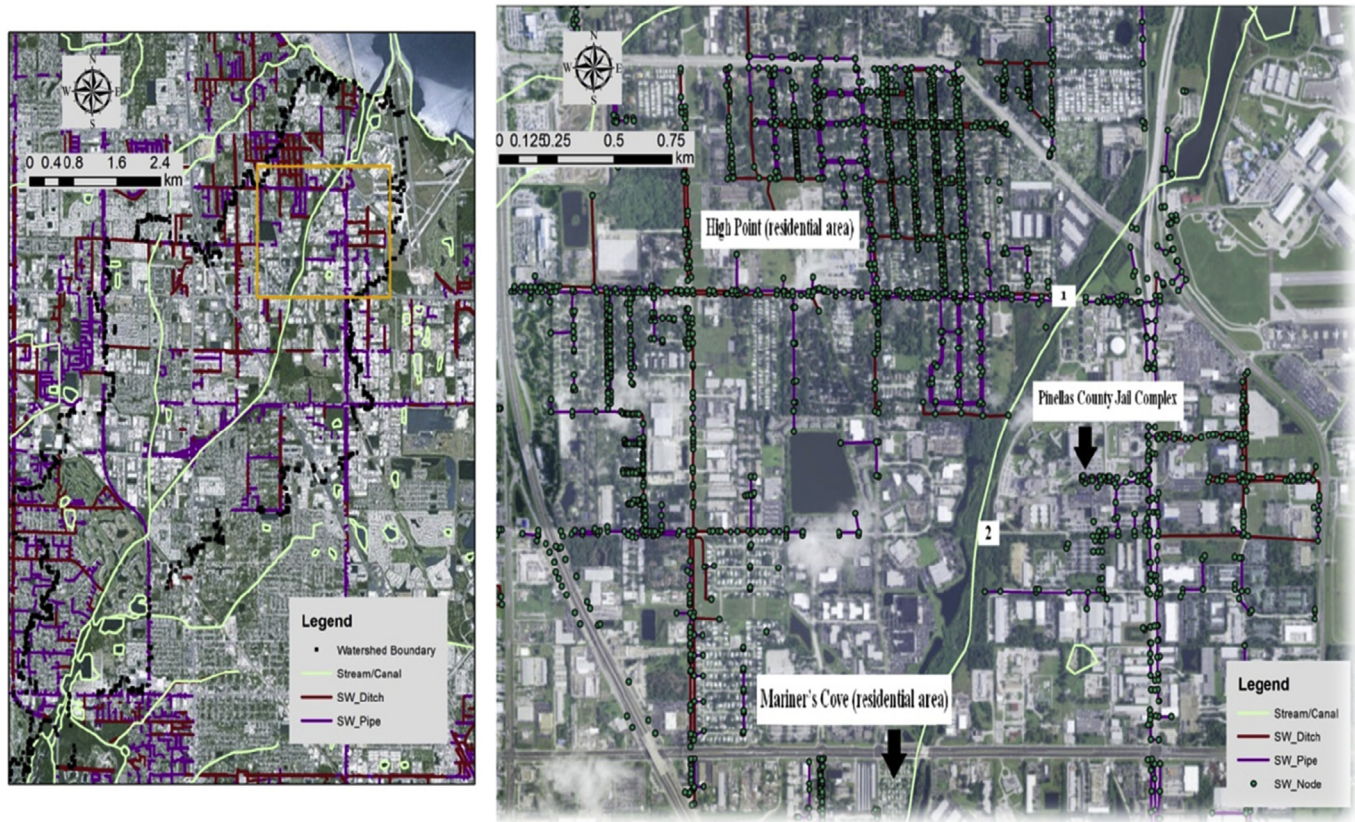


Fig. 5. Current drainage network and key points of outfall (1&2).

districts, and local governments. Local governments such as Pinellas County are the primary source for design storm considerations for LID implementation in the Cross Bayou watershed because it falls within county boundaries. In addition, Pinellas County also presents the largest of possible design storms with respect to stormwater management. Although magnitude is important in the design storm, duration is equally important. Qin et al. (2013) determined effects of LID on urban flooding at the urban drainage system scale under varying rainfall characteristics such as return period and duration. This analysis is useful because of the nature of rainfall in general and specifically for Florida, given the dominant rainfall types, convective and frontal. These convective and frontal events can be obtained from sub-daily hyetographs (Hernandez, 2001).

In addition, standardized rainfall distribution curves or rainfall mass curves can be created from hyetographs and used to represent the cumulative fraction of rainfall for a given duration and return period. These mass curves have been applied within watershed stormwater management design and are documented in the literature (Huff, 1967, 1990 and by the Soil Conservation Service, 1973). Mass rainfall curves can be developed specifically for convective and frontal storm scenarios, from both the historical period and the year 2030 in 15-min hyetographs, under a given return period and duration. Rainfall distributions of convective and frontal storm events at the sub-hourly scale can reveal much needed information about their potential runoff characteristics, respectively, particularly important for determining the effectiveness of reduced imperviousness via LID implementation across various sub-basins (Fig. 6). Table 4 summarizes methods for developing rainfall distributions for convective and frontal storms at the sub-hourly scale under given return period and duration.

3.4. Historical storm scenarios

Two known rainfall gauges (USGS 275021082450500 and NOAA/NWS/GHCND: USW00012873) exist within the Cross Bayou watershed; however, both gauges have varying periods of record. NOAA/NWS/GHCND: USW00012873 station provides the longest period of record (1998–present). The daily time scale presents challenges related to classifying convective and frontal rain events for analysis that require fine temporal resolution, 15 min or less. Alternatively, 15-min NEXRAD rainfall data were obtained from the Southwest Florida Water Management District (SWFWMD) with a 2 km × 2 km resolution (Fig. 7). The NEXRAD rainfall data period of record is from June 1995 to present.

In this study, from the historic and future rainfall predictions (Table 3), the first step consisted of developing daily hyetograph from the nearest rainfall gauge, the NOAA/NWS/GHCND: USW00012873 station near the St. Petersburg/Clearwater Airport. The second step was to determine the required design storm magnitude for a given duration. Because the Cross Bayou Watershed lies within Pinellas County boundaries, the Pinellas County stormwater manual was referenced to determine the design storm. Within the manual, a 25-yr, 24-hr storm (203–228 mm) was appropriate for open basins or drainage basins with discharge to a tidal waterbody, in this case the Cross Bayou Canal. The third and fourth steps plotted the design storm magnitude on the daily hyetograph from the rain gauge station and separated top daily storm(s), respectively (Fig. 8).

The fifth step consisted of developing sub-hourly hyetographs, such as 15-min temporal resolution, for the top daily storms determined in steps three and four. For this study, 15-min rainfall was obtained from the SWFWMD NEXRAD rainfall grid for each top

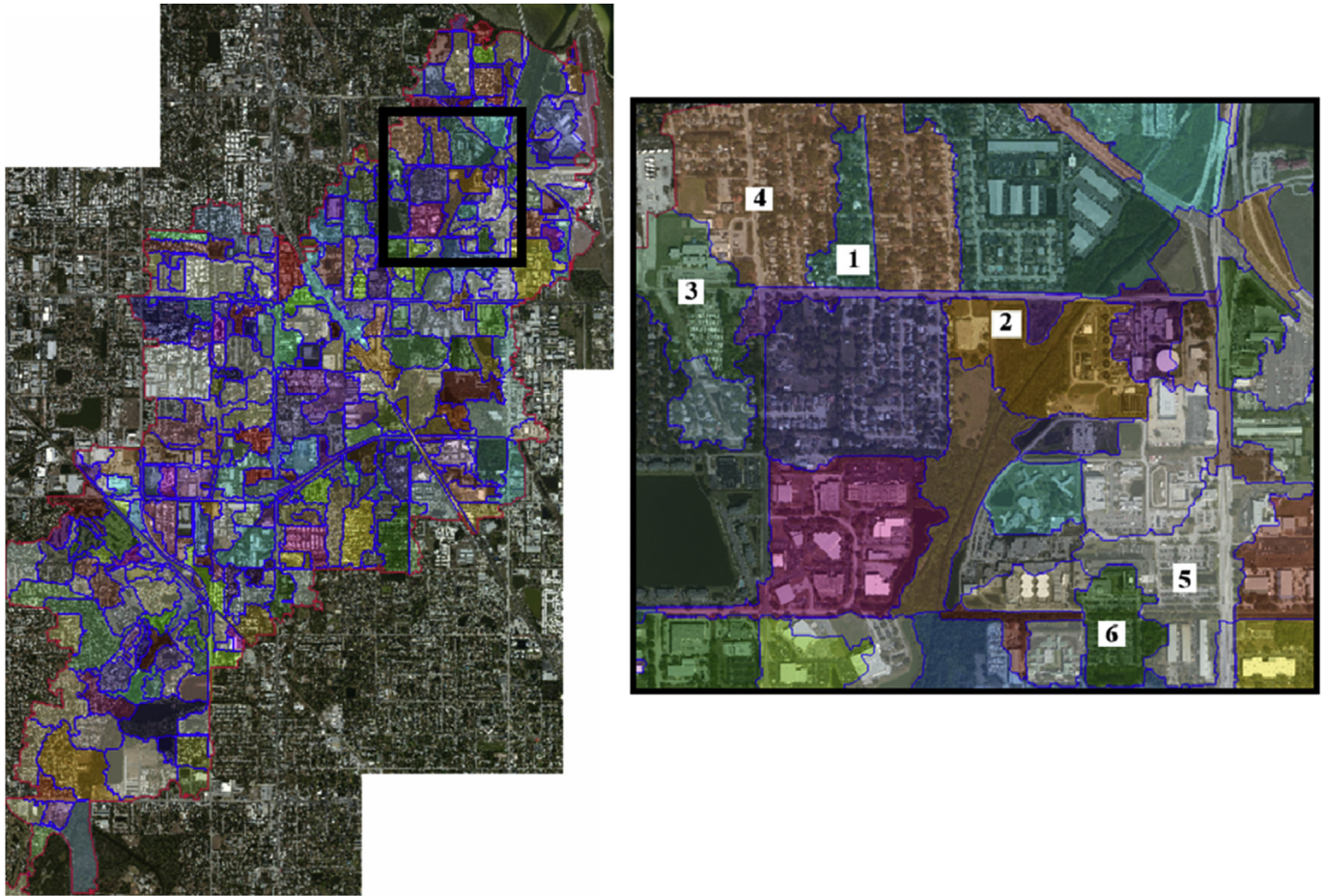


Fig. 6. Sub-basins within Cross Bayou Watershed for future LID implementation. Each color distinguishes each sub-basin.

Table 1
Percent Imperviousness & Perviousness for sub-basins in Fig. 8.

Basin No.	Basin size (acres)	Basin size (m ²)	Pre-LID % impervious	pre-lid % pervious
1	9.4	38,032	48.7	51.3
2	18.0	72,788	0.0	100.0
3	19.9	80,515	55.4	44.6
4	49.8	201,531	55.5	44.5
5	33.3	134,732	74.5	25.5
6	13.2	53,407	76.1	23.9

Table 2
Scenarios for Imperviousness Reduction in the proposed LID Portfolio.

Basin No.	Existing % imperviousness	Scenario 1		Proposed LID
		25% reduction in imperviousness	50% reduction in imperviousness	
1	48.7	36.6	24.4	Swales
2	0.0	0.0	0.0	Retention Pond
3	55.4	41.5	27.7	Green Roof, Swales, Pervious Pavement
4	55.5	41.6	27.8	Green Roof, Swales, Pervious Pavement
5	74.5	55.9	37.3	Green Roof, Swales, Pervious Pavement
6	76.1	57.0	38.0	Pervious Pavement

daily storm (Fig. 9). Discrepancy was noted for the July 18, 2004, storm between the daily rain gauge and the NEXRAD grid. The 15-min NEXRAD hyetograph intensity for the July 18, 2004 storm was less than expected as compared to the daily rainfall gauge possibly indicating that the July 18 event was a highly localized convective

storm with varying intensity throughout the 2 km × 2 km grid area. For this study, the July 18, 2004, event was omitted from further analysis while the remaining storms were kept for consideration.

The sixth step consisted of information from step five (Fig. 9) to determine convective and frontal rainfall characteristics. With the

Table 3
LID design storm approach across varying levels of governance.

Level of governance	Agency/Governing body	Design storm for stormwater management	Specific to LID/BMP?	Reference
National	Environmental Protection Agency (EPA) Regional Frequency Analysis using L-moments	2-, 10- and 100-yr storms 1-yr, 2-yr, 5-yr, 10-yr, 25-yr, 50-yr, 100-yr, 200-yr, 500-yr and 1000-yr 15-min, 30-min, 1*, 2*, 3*, 6*, 12*, 1**, 2-**, 3**, 4**, 7**, 10**, 20**, 30**, 45** and 60**	Yes	Clar et al. (2004) NOAA (2013) Hosking and Wallis (1997)
State	Florida Department of Environmental Protection (FDEP)	3-yr 1-hr storm	Yes	Florida Department of Environmental Protection (2014)
District	Southwest Florida Water Management District (SWFWMD)	25-yr event in an open basin or the 100-yr event in a closed basin	Yes	SWFWMD (2013)
County	Pinellas County	100-yr, 24-hr	Yes	Pinellas County (2016)

Note: (*) represents hour and (**) represents days.

Table 4
Developing rainfall distributions for convective and frontal storms under given return period and duration.

Step	Historical period	Future period
1	Develop daily hyetograph(s) for a given historical period	Develop daily hyetograph(s) for a future period of concern
2	Determine required design storm magnitude for a given duration [i.e. (N)-yr (X)-hr storm]	Determine required design storm magnitude for a given duration [i.e. (N)-yr (X)-hr storm]
3	Plot design storm magnitude on the daily hyetograph for period of concern and determine the top daily storms near design storm magnitude	Plot design storm magnitude on the daily hyetograph for period of concern and determine the top daily storms near design storm magnitude
4	Separate top daily storm(s)	Separate top daily storm(s)
5	Determine top storm(s) 15-min rainfall patterns using historical record or disaggregation methods	Determine top storm(s) 15-min rainfall patterns using disaggregation methods
6	Determine convective and/or frontal patterns from top storm(s) 15-min hyetographs	Determine convective and/or frontal patterns from top storm(s) 15-min hyetographs

exception of the storm on July 18, 2004, the storm on June 24, 2012, indicated a much larger variability within periods of short duration and a slightly higher intensity (Fig. 9), indicating a highly convective storm nature. The storm on February 3, 2006, although indicative of maximum intensity close to that of the storm on June 24, 2012, did not exhibit large variability within a short duration. Although the storm on February 3, 2006, began with higher intensity, the storm intensity decreased and remained between 5 and 10 mm throughout midday. From this information, this particular

storm may indicate a frontal pattern. From step six, rainfall distribution curves (Fig. 10) can be developed for both the top convective and frontal storms (with the exception of the July 18, 2004, storm). These curves define the historical storm scenarios used to determine the effectiveness of reduced surface imperviousness via LID implementation under the historical period only.

3.5. Future storm scenarios (Year, 2030)

Future 15-min rainfall hyetographs were created using daily observed rainfall, statistical climate modeling, and rainfall disaggregation methods. The Statistical Downscaling Model (SDSM) (Wilby et al., 2002) is useful in this regard and was applied to determine statistical relationships, based on multiple linear regression techniques, between large-scale climate variables and local climate. These relationships were developed using observed weather data and the Global Climate Model (GCM) derived atmospheric predictors to obtain local climate information for some future time period, the year 2030 for this study. Daily observed climate data (predictands) are required inputs for SDSM, with the predictand of importance being daily rainfall. Because multiple linear regression is used within SDSM, users typically would need observed data as close to normal distribution as possible. Because daily rainfall is typically positively skewed, a transformation of the data was required to obtain a near-normal distribution, achieved using the log transformation of observed rainfall data.

In addition to daily climate input, another important component of SDSM is predictor variables used to describe state of the climate for a particular period of analysis. Selecting the best predictors is a trial and error process to remove the least significant predictors until the remaining predictors are statistically significant, establishing a clear relationship between predictor variables and predictands, such as rainfall. Predictor variables utilized in SDSM for this study were derived from the Hadley Center Coupled Model, version 3 (HADCM3) GCM A2 scenario of the Intergovernmental

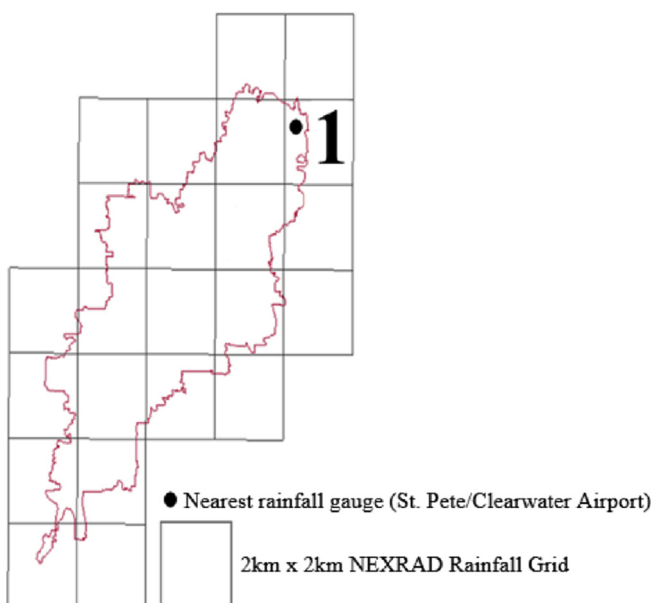


Fig. 7. 2 km × 2 km SWFWMD NEXRAD rainfall grid cells over the watershed with the location of a daily rain gauge.

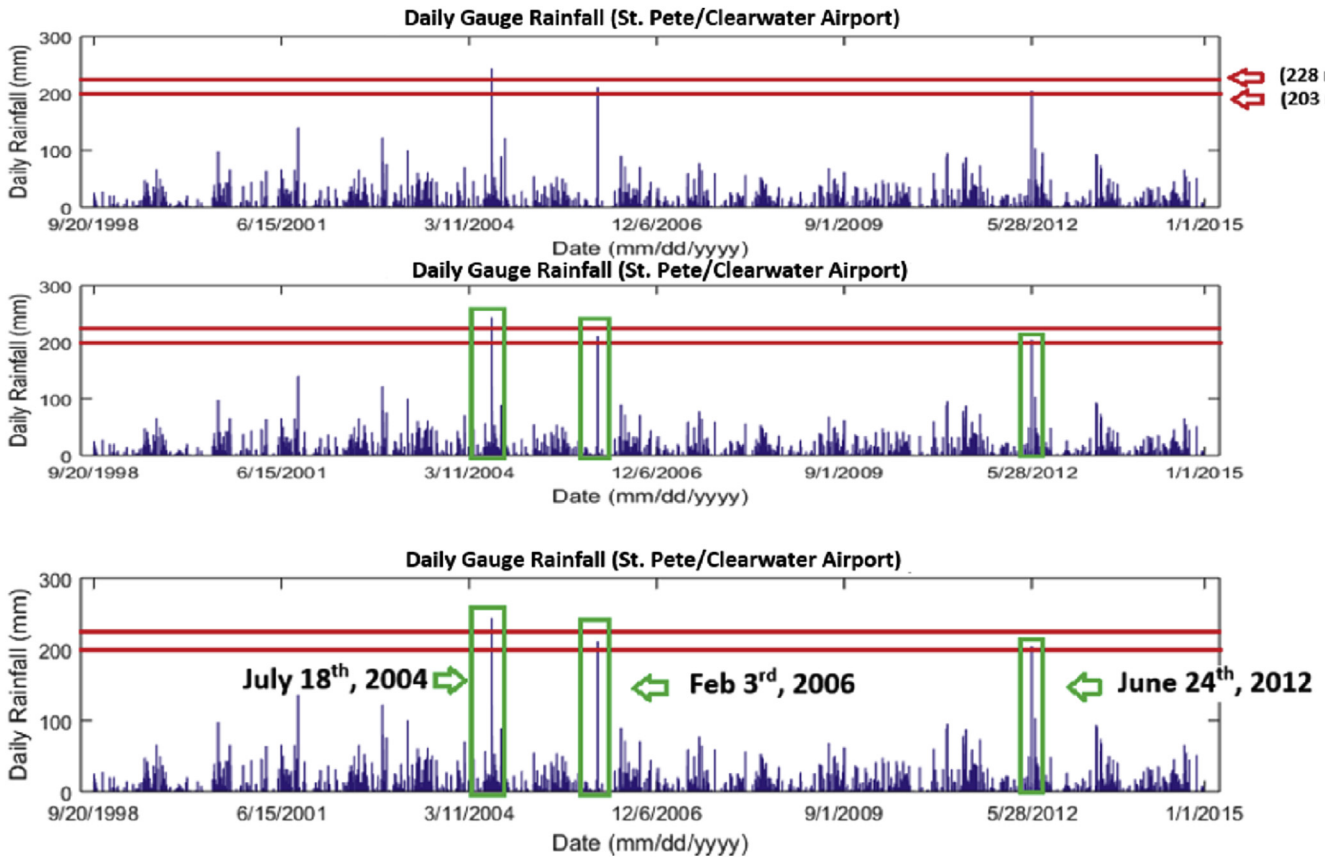


Fig. 8. Separating top storm(s) within a given design storm magnitude range.

Panel on Climate Change Fourth Assessment Report (IPCC, 2014). All atmospheric predictor variables were re-gridded to a standard coordinate system (2.5° latitude × 3.75° longitude) used in HADCM3 covering 1961 to 2099 (Appendix B).

Validation of SDSM focused on how SDSM can capture mean monthly rainfall compared with observed. Although it is important for SDSM to capture the mean monthly rainfall during validation, it is equally important for SDSM to capture monthly variance within the validation period. The ability of SDSM to capture the monthly variance within the validation period is important for this study because of the need to capture variation in rainfall patterns as opposed to only mean rainfall (Appendix B).

Because input and output data were on a daily scale in SDSM, disaggregation methods were needed to provide estimates of future rainfall on a sub-hourly scale or 15-min increments. Given a wide variety of disaggregation methods available for disaggregating rainfall (Koutsoyiannis et al., 2003; Wey, 2007; Zhang et al., 2008) across various temporal resolutions, a more recent method, the method of fragments, has been a useful in particular case studies (Pui et al., 2012; Westra et al., 2012). The method of fragments (Equation (1)) relies on a set of fragments, which are a fraction of the temporal resolution desired for disaggregation.

$$F_i = \frac{X_i}{\sum_{i=1}^n X_i} \quad (1)$$

where,

- F_i is the fragment at disaggregated time scale;
- X_i represents the data at the disaggregated time scale.

The computed fragments become factors multiplied by generated data of the temporal resolution to be disaggregated (Equation (2)).

$$X'_i = F_i * I \quad (2)$$

where,

- X'_i represent the data at the disaggregated time scale;
- I represent the generated data at the temporal resolution to be disaggregated;
- F_i represent the fragment at disaggregated time scale.

For this study, the computed fragments are at the disaggregated time scale of 15-min, and the data being disaggregated is the daily rainfall from SDSM for the year 2030. The series of 15-min data used to compute the 15-min fragments were determined by comparing the 15-min rainfall hyetographs within the watershed boundary with 15-min rainfall hyetographs outside the watershed boundary that sum to near the 25-yr, 24-hr design storm magnitude (203–228 mm). The goal is to observe changes in sub-daily rainfall patterns with respect to watershed boundary distance. The distribution of 15-min rainfall for the February 3, 2006 (Figs. 11 and 12) and June 24, 2012 (Figs. 13 and 14) rainfall events were determined for two different locations.

Similarly, for the historical period storm analysis, the first step for future storm scenarios is to obtain a daily hyetograph for year 2030 to determine storm(s) within the design storm magnitude range. A daily hyetograph for 2030 was produced using SDSM under the HADCM3 global climate model A2 scenario, highlighting the three best series of a 20-member SDSM ensemble (Fig. 15).

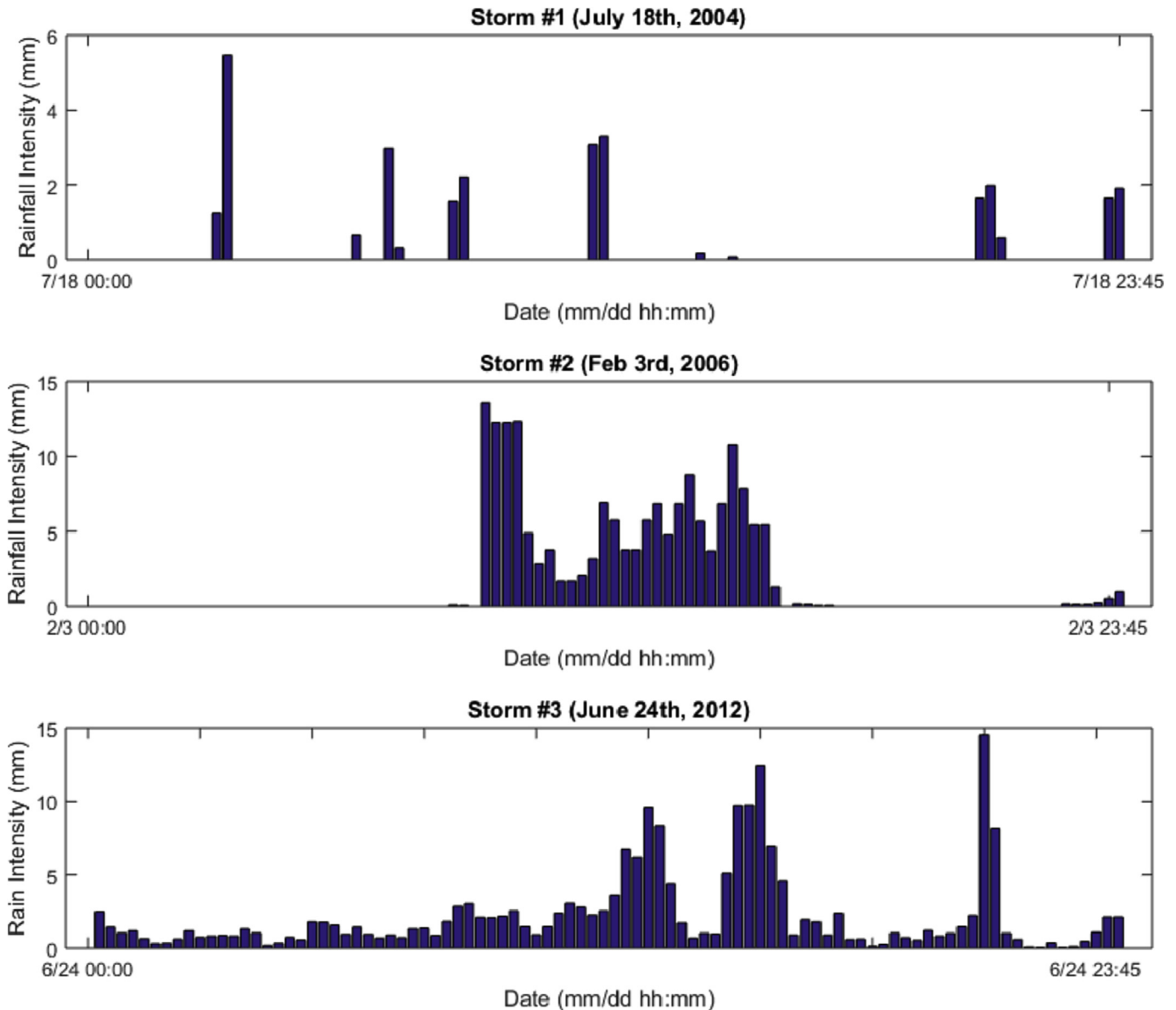


Fig. 9. 15-min hyetographs of top daily storms determined from Fig. 10. Note: Storm #1 was not used in analysis due to discrepancy in radar and gauge measurements.

The second step is to determine the required range of design storm magnitude for a 25-yr, 24hr storm that is the same as for the historical period storm scenarios. The third and fourth steps are to plot the design storm magnitude on the daily hyetograph from the rain gauge station and separate top daily storm(s), respectively (Fig. 16). Series 3 was chosen because more than one top storm could be used. Because of significant bias for December in the SDSM validation, December storms were not considered.

From Fig. 16, the May 27, 2030 storm is classified as a frontal storm while the October 15, 2030, is classified as a convective storm event since frontal events typically dominate from November to May whereas convective events dominate from June to October (Ali et al., 2000). The fifth step consists of developing sub-hourly hyetographs at 15-min temporal resolution, similar to historical period storm scenarios, for the top daily storms determined in steps three and four. In contrast to the fifth step for historical period storm scenarios, this step requires rainfall disaggregation of daily SDSM

rainfall, accomplished using the method of fragments as previously discussed. The development of 15-min resolution fragments of the daily May 2030 frontal storm use the hyetographs from Figs. 11 and 12 whereas the daily October 2030 convective storm uses hyetographs from Figs. 13 and 14 to develop similar 15-min fragments.

3.6. Sea level rise (SLR)

Estimating future tide levels in the Cross Bayou tidal canal required selecting a daily time series with the highest tide levels and determining the relative sea level change for 2030 with respect to the year with the highest recorded tide levels. The intermediate-high scenario of NOAA sea level rise projections, noting a projected warming of the ocean and ice sheet loss globally, was used to determine the relative sea level change (Tampa Bay Climate Science Advisory Panel, 2015).

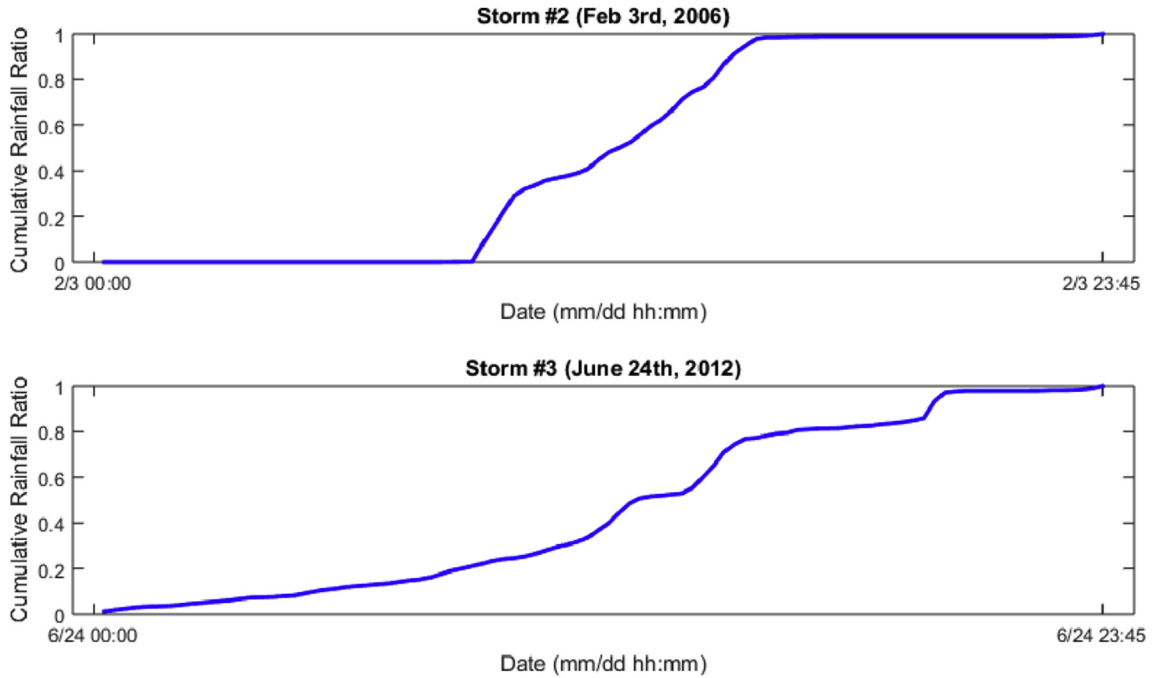


Fig. 10. Cumulative rainfall curves for top convective (bottom) and frontal storms (top) from historical period.

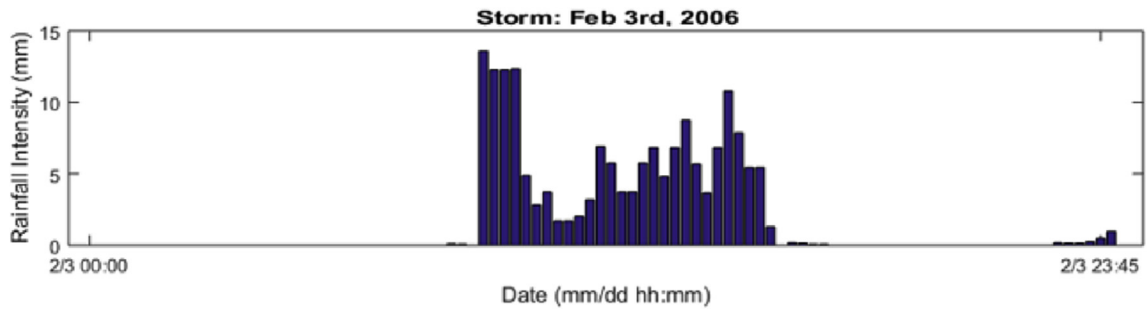


Fig. 11. 15-min hyetographs for February 3rd, 2006 storm (frontal event) within the watershed boundary [Will be denoted hereafter as frontal rainfall pattern #1].

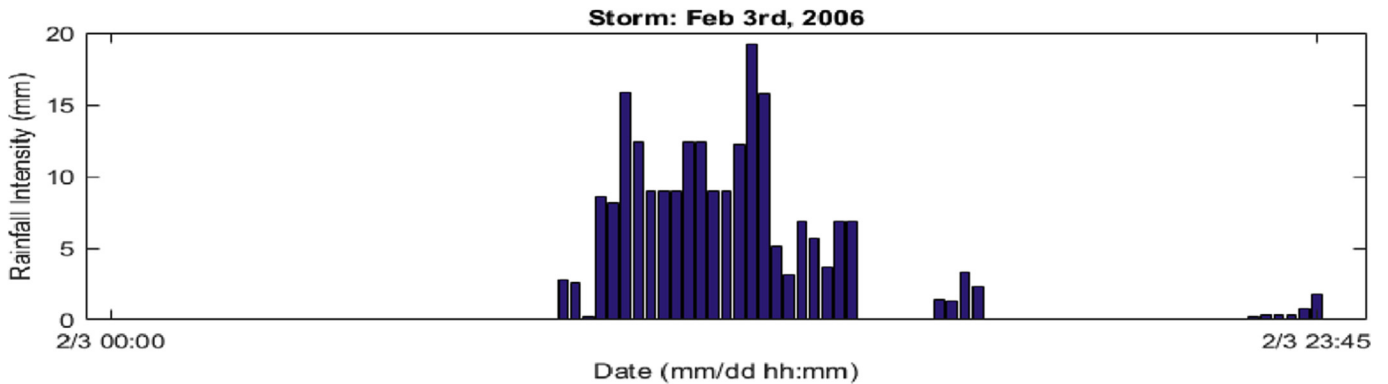


Fig. 12. 15-min hyetographs for February 3rd, 2006 storm (frontal event) approx. 4 km from nearest watershed boundary. [Will be denoted hereafter as frontal rainfall pattern #2].

3.7. Quantitative metrics

Inflow rate reduction was a key quantitative metric in this study for characterizing effectiveness of LID implemented in reducing runoff in relation to existing conditions. Inflow rate reduction was determined using the following expression for both historical and

future convective storm scenarios:

$$\frac{\text{Existing Inflow Rate} - \text{LID Scenario Inflow Rate}}{\text{Existing Inflow Rate}} * 100\% \quad (3)$$

where,

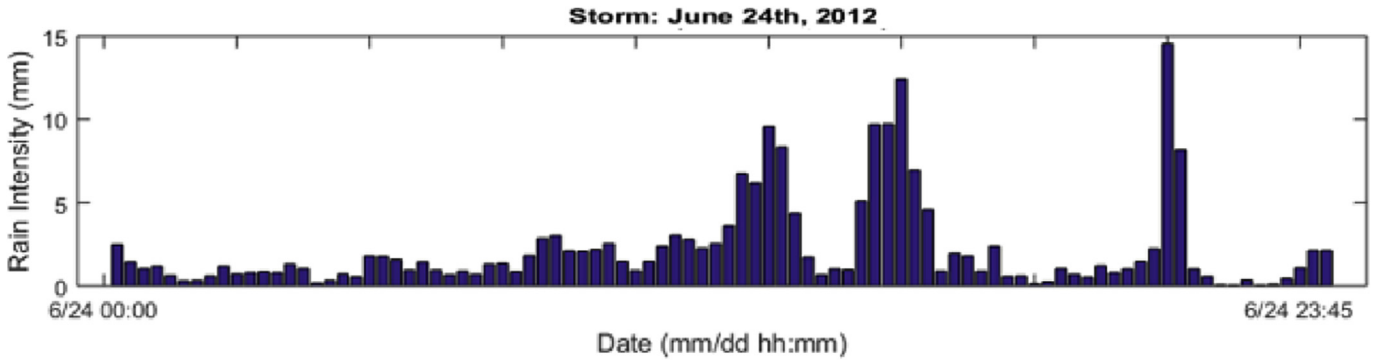


Fig. 13. 15-min hyetographs for June 24th, 2012 storm (convective event) within the watershed boundary. [Will be denoted hereafter as convective rainfall pattern #1].

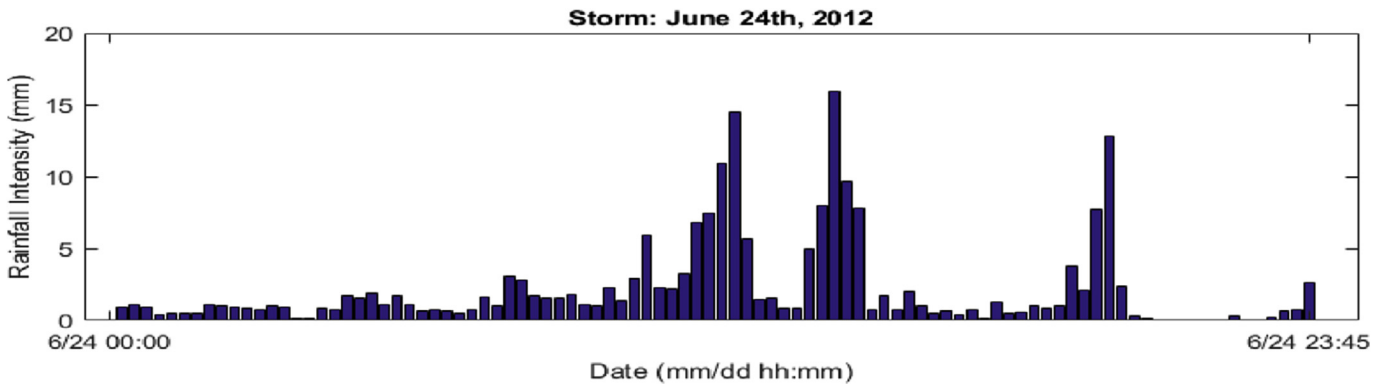


Fig. 14. 15-min hyetographs for June 24th, 2012 storm (convective event) approx. 4 km from nearest watershed boundary. [Will be denoted hereafter as convective rainfall pattern #2].

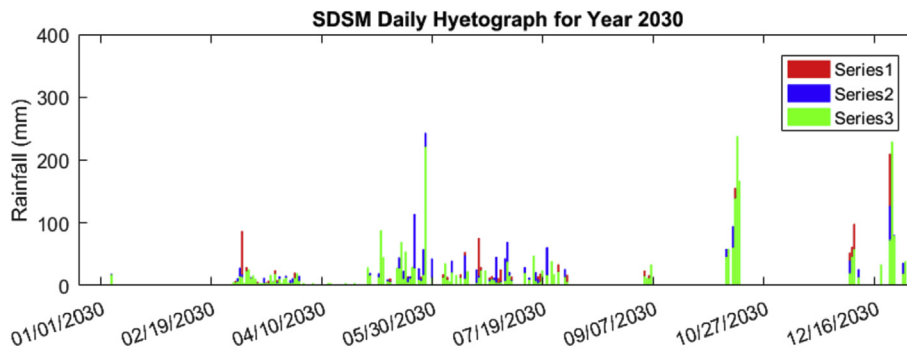


Fig. 15. Daily SDSM rainfall hyetograph for the year 2030 for three-time series.

Existing Inflow Rate = Inflow at a specific location based on existing infrastructure;
 LID Scenario Inflow Rate = Inflow at a specific location under LID scenario(s) (1 & 2).

Inflow rate reduction was determined at five locations (Fig. 17) during both the historical period and future period. Inflow rates were determined using a comprehensive hydrological and hydraulic model, the ICPR software.

4. ICPR4 model

The ICPR4 model is a comprehensive hydrodynamic stormwater and hydrologic model that incorporates hydroinformatics and geoinformatics along with input for climate data and processing.

ICPR was utilized to construct a detailed model of the Cross Bayou watershed, which includes an integrated surface and groundwater interface. ICPR integrates terrain data, hydrologic data, hydraulic data, and climate data via a layering and data management system (Fig. 18).

4.1. Urban hydroinformatics

To determine the resiliency of the green-grey stormwater drainage system with respect to both current and future hazards, extensive data collection and processing of the stormwater drainage network was required. Urban hydroinformatics applies the concept of hydroinformatics (Abbott, 1991) to urban water management, which includes urban water systems such as stormwater networks. Its application has addressed needs for managing

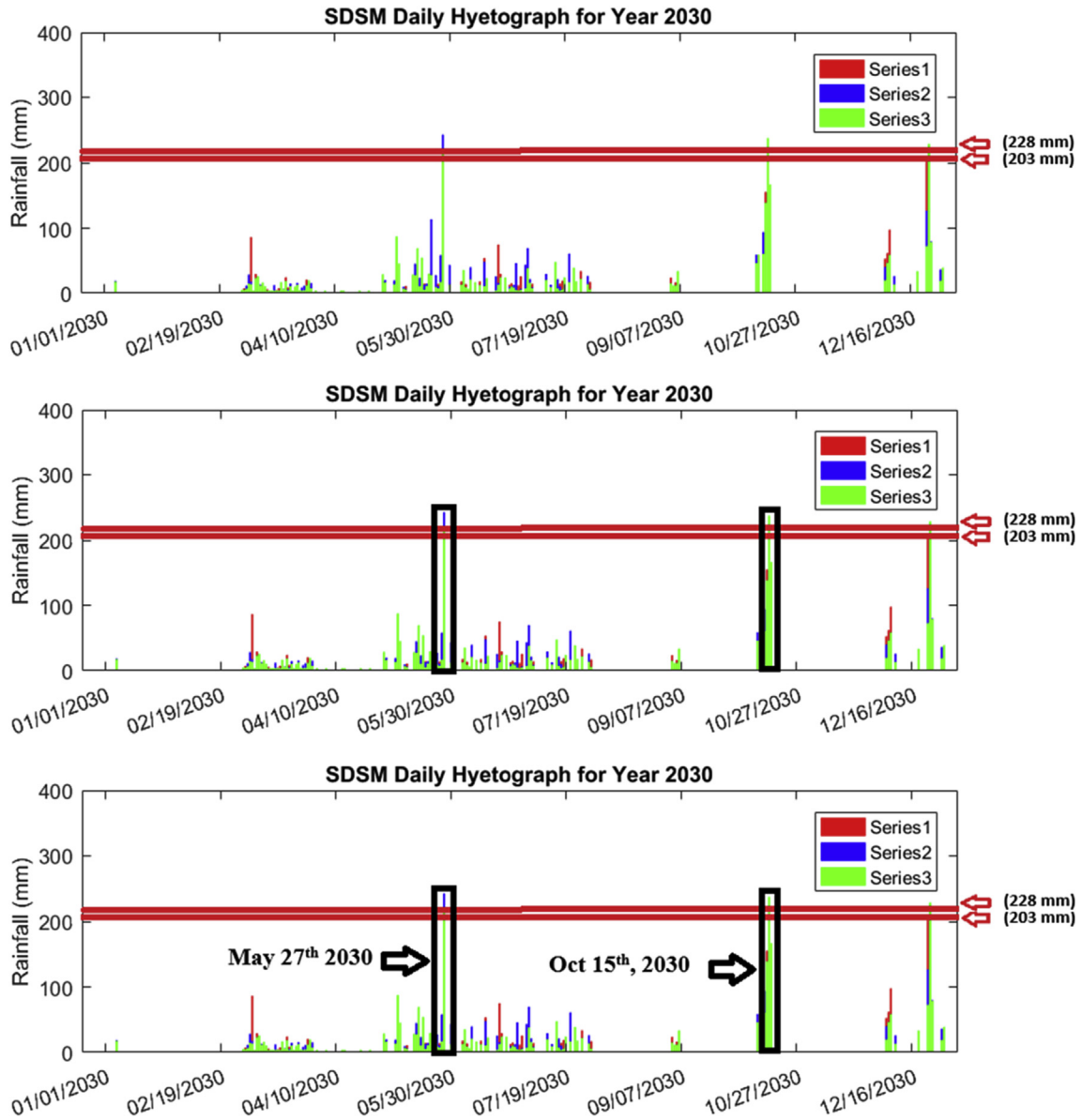


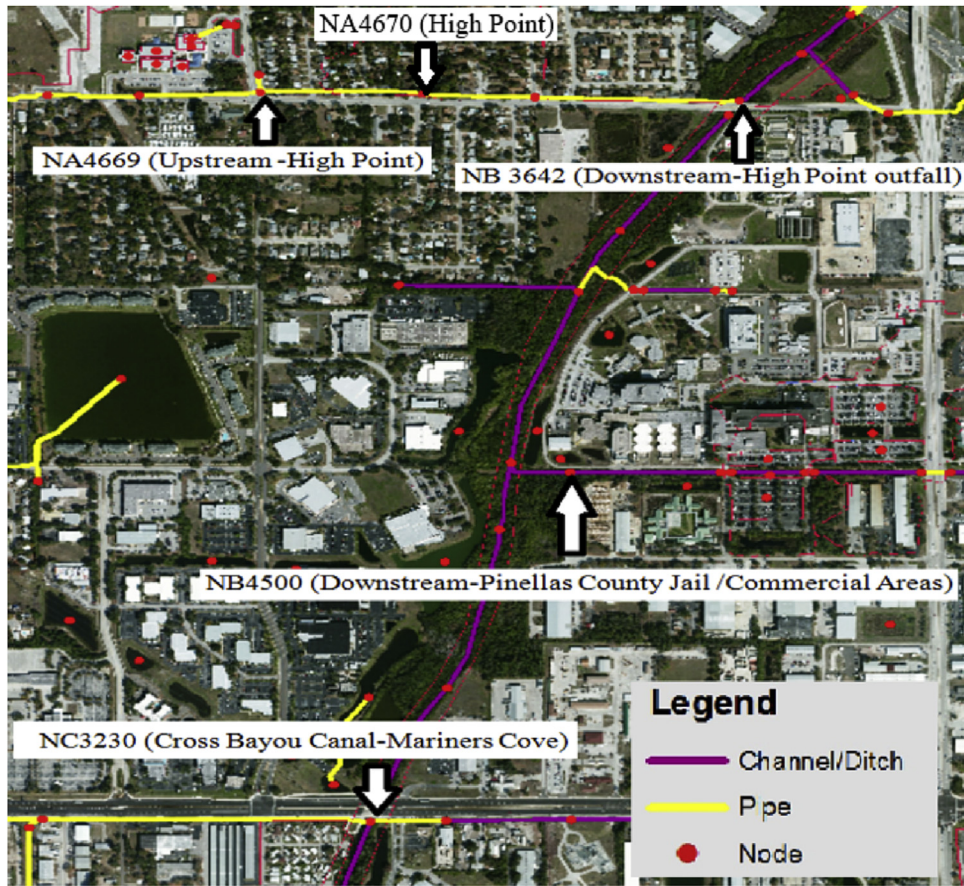
Fig. 16. Separating top storm(s) within a given design storm magnitude range across three SDSM daily time series for the year 2030.

flow of water in the urban environment. With the use of detailed, physically based models, there is an increasing need for models to utilize and manage extensive, spatially referenced databases. In highlighting the role of urban hydroinformatics in urban flood management, Price and Vojinovic (2008) reported one of the most important factors in success of modeling analyses: the ability of a model to acquire data to improve information and understanding about described physical processes.

A survey of significant hydraulic conveyance features in the watershed, including channels, culverts, drop inlets (rise culverts), overland weirs, and structural weirs, was provided by an analysis conducted in the Cross Bayou Watershed Management Plan for Pinellas County (Jones Edmunds and Associates, Inc., 2013). These conveyance features were collected, organized, and managed within the ICPR4 model for further processing and utilization. From this information, a model of the existing drainage was constructed, focusing on major conveyance features and outfalls. More complex drainage systems found in the watershed were incorporated in

time of concentration, or time it takes for runoff to travel from the most hydraulically distant point in the watershed to an outlet point, using the National Resources Conservation Service (NRCS) method for small urban watersheds (Natural Resources Conservation Service, 1986).

The hydrology of the Cross Bayou ICPR4 model consists of traditional basins (mapped and manual as specified in ICPR). The mapped basins are georeferenced polygons that integrate traditional hydrology (i.e., NRCS unit hydrographs with times of concentration) allowing interaction with groundwater via recharge. Manual basins are basins in the ICPR model that do not interact with the groundwater. Green-Ampt infiltration was considered for each sub-basin based on the soil characteristics from the NRCS soil survey (Appendix C). Mapped basins were developed from preliminary sub-basin (catchment) delineations for the Cross Bayou watershed in accordance with the SWFWMD guidelines and specifications. The total number of sub-basins in the watershed was limited to approximately 300. Sub-basins were delineated around



Note:

1. Node NA4669-Runoff collected at major conveyance point in High Point
2. Node NA4670-Runoff collected at major conveyance point in High Point
3. Node NC3642-Runoff into the Cross Bayou Canal from High Point conveyance systems
4. Node NB4500-Runoff from areas surrounding the Pinellas County Jail complex
5. Node NC3230-Combined tidal flows and discharge to Cross Bayou Canal near Mariners Cove

Fig. 17. ICPR drainage outfalls for analysis.

all major drainage conveyances and significant detention systems and at other locations as required to supply adequate definition to the model (Jones Edmunds and Associates, Inc., 2013).

The Green-Ampt parameters were assumed using a typical soil class (Appendix C) for the area with no recharge to the surficial aquifer beneath the area of concern. Two manual basins were included in the Cross Bayou model to estimate offsite flow contributions into the watershed from St. Joes Creek and Pinellas Park Ditch. Times of concentration for these two basins were approximated based on the longest flow path with an assumed travel time of 0.305 m s^{-1} (1 ft s^{-1}). Because these basins are highly developed or urbanized, the impervious area was assumed to be 65%, with 45% directly connected to impervious area.

In the hydraulic component of the model, major drainage conveyances deemed as part of the grey drainage infrastructure were placed in the model ICPR using a one-dimensional (1D) form of the momentum equation along with energy and diffusive wave options and averaged 2D ground slopes to move water between control volumes via the overland flow links. For this study, the 2D

momentum equation was used to calculate overland flow, and the 1D energy equation was used to calculate flow within channels and other hydraulic systems such as the storm sewer system. ICPR4 was applied for the Cross Bayou watershed study and was well calibrated and validated based on a series of storm events with the aid of two USGS gauge stations (Appendix B). The energy equation used for hydraulics can be represented as follows:

$$Z_1 + \frac{V_1^2}{2g} = Z_2 + \frac{V_2^2}{2g} + h_f \quad (4)$$

Solving for Q:

$$Q = \left\{ \frac{Z_1 - Z_2}{\frac{1}{2g} \left[\frac{1}{A_2^2} - \frac{1}{A_1^2} \right] + \Delta x C_f} \right\}^{1/2} \quad (5)$$

where Q = flow (m^3s^{-1}); Z_1 = elevation (m) at node 1;

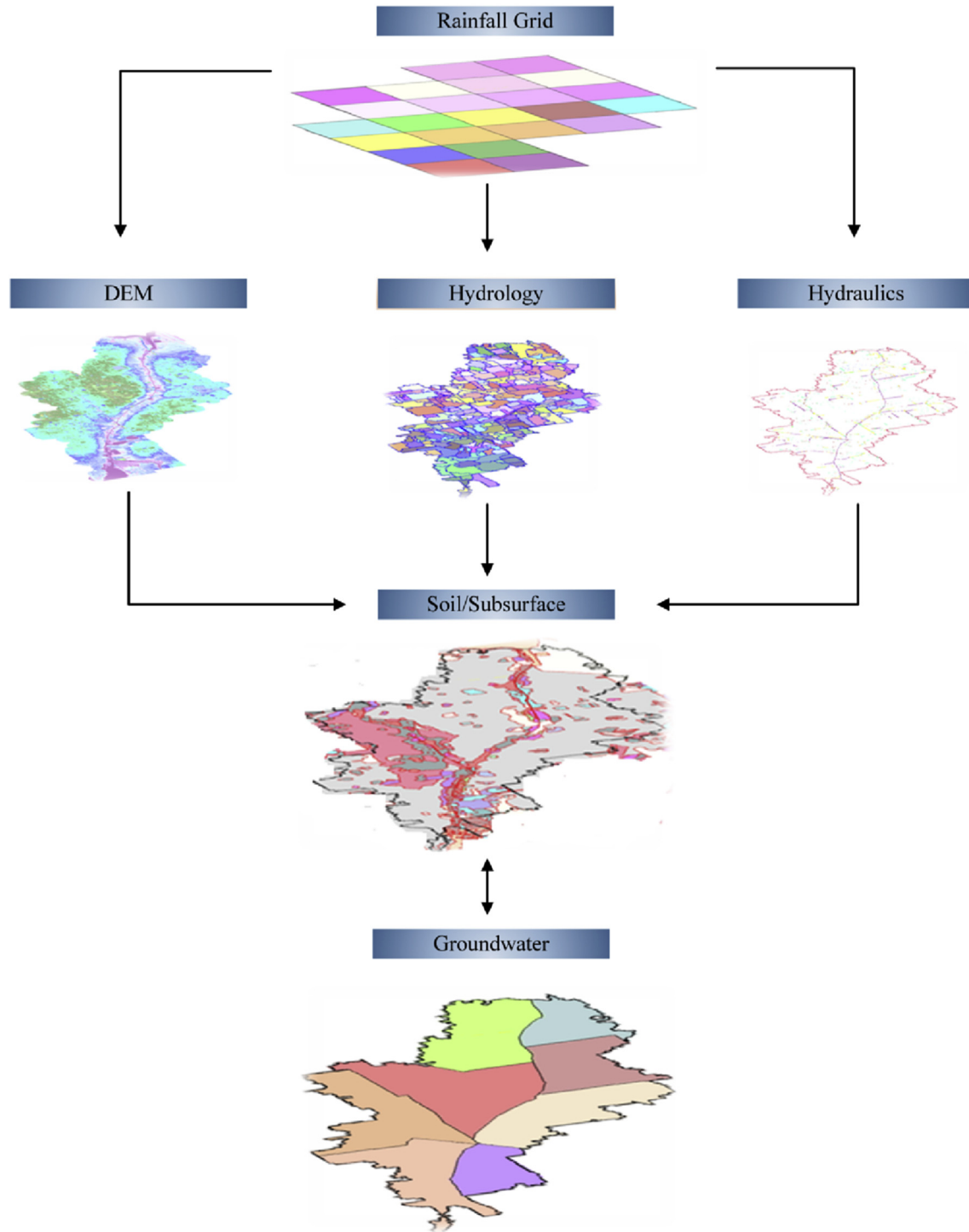


Fig. 18. Flow of information between primary ICPR data layers.

Z_2 = elevation (m) at node 2; Δx = change in length between nodes in the x-direction; g = gravitational acceleration ($m\ s^{-2}$); A_1 = cross sectional area (m^2) at node 1; A_2 = cross sectional area (m^2) at node 2; C_f = coefficient of friction;

The energy equation is modified for channel and pipe flow and can be represented as follows:

$$Z_1 + \frac{\alpha_1 V_1^2}{2g} = Z_2 + \frac{\alpha_2 V_2^2}{2g} + h_f + h_{eddy} + h_{entrance} + h_{exit} + h_{bend} \quad (6)$$

Solving for Q:

$$Q = \left\{ \frac{Z_1 - Z_2}{\frac{1}{2g} \left[\left(\frac{\alpha_2}{A_2^2} - \frac{\alpha_1}{A_1^2} \right) C_{eddy} \left| \left(\frac{\alpha_2}{A_2^2} - \frac{\alpha_1}{A_1^2} \right) \right| + \left(\frac{\alpha_1 C_{entrance}}{A_1^2} \right) + \left(\frac{\alpha_2 C_{exit}}{A_2^2} \right) + \left(\frac{\alpha_{bend} C_{bend}}{A_{bend}^2} \right) + \Delta x C_f \right]} \right\}^{1/2} \quad (7)$$

where

Q = flow ($\text{m}^3 \text{s}^{-1}$); Z_1 = elevation (m) at node 1; Z_2 = elevation (m) at node 2;

Δx = change in length between nodes in the x-direction;

g = gravitational acceleration (m s^{-2});

A_1 = cross sectional area (m^2) at node 1; A_2 = cross sectional area (m^2) at node 2;

A_{bend} = area of the bend (m^2); α_1 = energy loss coefficient at node 1;

α_2 = energy loss coefficient at node 2; C_f = friction loss coefficient; C_{eddy} = eddy loss coefficient;

$C_{entrance}$ = entrance loss coefficient; C_{exit} = exit loss coefficient; C_{bend} = bend loss coefficient;

Mass balance equations are utilized within the control volumes at each node as follows:

$$dz = \left[\frac{\sum(Q_{in} - Q_{out})}{A_{surface}} \right] dt \quad (8)$$

where

dz = incremental change in stage (m); dt = computational time step (s);

Q_{in} = total inflow rate ($\text{m}^3 \text{s}^{-1}$); Q_{out} = total outflow rate ($\text{m}^3 \text{s}^{-1}$); $A_{surface}$ = wetted surface area of control volume and

$$Q_{in} = \sum Q_{link\ in} + \sum Q_{excess} + \sum Q_{external} + \sum Q_{seepage} \quad (9)$$

$$Q_{out} = \sum Q_{link\ out} + \sum Q_{irrigation} \quad (10)$$

where

$\sum Q_{link\ in}$ = sum of all link flow rates entering the control volume ($\text{m}^3 \text{s}^{-1}$);

$\sum Q_{link\ out}$ = sum of all link flow rates leaving the control volume ($\text{m}^3 \text{s}^{-1}$);

$\sum Q_{excess}$ = sum of rainfall excess rates for all basin polygons ($\text{m}^3 \text{s}^{-1}$);

$\sum Q_{external}$ = sum of inflows from all external sources ($\text{m}^3 \text{s}^{-1}$);

$\sum Q_{seepage}$ = sum of seepage flow from groundwater model ($\text{m}^3 \text{s}^{-1}$);

$\sum Q_{irrigation}$ = sum of irrigation water pulled from surface node ($\text{m}^3 \text{s}^{-1}$)

A 2D overland flow region was created to allow the groundwater components to interact with surface water components through an overland flow region in the model. This interaction occurred below the specified sub-basins and within pond and channel control volumes as specified in the model. Eight groundwater regions were created within the ICPR4 model. Groundwater region boundaries were defined by channel features that were typically inundated. As water infiltrates the ground surface, a known head condition was placed at the corresponding groundwater nodes, derived from

water surface elevations in the surface model component of the model.

4.2. Geoinformatics

Geoinformatics involves the use of information science to acquire, store, and manage geospatial data, particularly important for hydrologic models because many depend on georeferenced, high spatial resolution data and information. To construct a reliable model of the Cross Bayou watershed, extensive geospatial data collection and assimilation was needed, including elevation data over the study region, soil data maps, and land use maps, provided by the Pinellas County government, Streamline Technologies, and Jones Edmunds & Associates Inc. The Natural Resources Conservation Service (NRCS) digital soil survey was utilized to develop the initial Green-Ampt soil parameters for the vadose zone and the surficial/unconfined aquifer within the watershed. A $1.5 \text{ m} \times 1.5 \text{ m}$ ($5 \text{ ft} \times 5 \text{ ft}$) ground digital elevation model (DEM) was used to define the ground surface of the watershed.

Because the DEM lacked accuracy below the water surface, and groundwater considerations were necessary for analysis, an “engineered” surface was created that projected the bottom elevation of known water bodies to well below sea level to prevent artificial drying of the water body. For the groundwater component of the hydrodynamic stormwater and hydrologic model, DEMs were also created for the initial water table elevation, based on wet season conditions as defined in the NRCS soil survey and the top of the confining layer for the Intermediate Aquifer System (IAS). The IAS includes all aquifers between the overlying surficial aquifer and the underlying Floridian aquifer. The initial water surface DEM was based on the NRCS depth to water table information. The IAS confining layer top elevation was obtained from a $390 \text{ m} \times 390 \text{ m}$ DEM based on contours generated using both automated and manual methods from the Florida Geological Survey (Streamline Technologies Inc., 2015). The geospatial data were embedded into a geographic information systems framework with corresponding layers and metadata to be accessible within the ICPR4 model.

4.3. ICPR model calibration & verification

For model calibration and verification, 15-min USGS gauge data were collected at the two active gauges within the Cross Bayou watershed (Appendix D). USGS gauge 02308870 is located along the Pinebrook Canal at Bryan Dairy Road in Pinellas Park. The gauge records rainfall and stage and flow data. The second USGS gauge 02308861 is located along Cross Bayou at Cedar Brook Drive in Pinellas Park. This gauge only records stage data. The stage data are relative to a local datum for the gauge. A conversion of 0.274 m (+0.9 ft) was used to convert the stage elevation from the local datum to NAVD88. The gauge period of record for rainfall, stage, and flow were August 6, 1999, to present; August 5, 1995, to present; and August 1, 1999, to present, respectively. Fifteen-minute NEXRAD rainfall data were obtained from the SWFWMD and distributed over 23 cells with $2 \text{ km} \times 2 \text{ km}$ grids from June 6, 1995, to December 31, 2014. Historical hourly tide gauge data from

January 1995 to December 2014 recorded at nearby NOAA tide stations were also used in calibration and verification of the model.

Daily reference evapotranspiration (ET) data from June 1, 1995, to December 31, 2013, were collected from the United States Geological Survey and distributed on 2 km × 2 km grid tiles. Specific to the ICPR model, crop coefficients were used to adjust reference ET to specific vegetation. A generalized crop coefficient map layer was created based on vegetation coverage. Although defined crop coefficients do not include impervious areas, they were used to describe vegetation types for pervious areas. Seven vegetative classes were established within the layer. The Green-Ampt method was used for infiltration and rainfall excess computations. The Green-Ampt parameters were developed based on the NRCS digital soils data and later adjusted during the calibration process (Appendix C). For each sub-basin, an initial abstraction parameter for impervious areas was set to 0.05 inches based on calibration of the model.

ICPR was calibrated using both a single historical storm event

(June 21–30, 2012) and verified using a long-term simulation between January 1, 2007, and January 1, 2014, using USGS gauging stations within the Cross Bayou Watershed. Years 2007 and 2008 were considered “warm-up” years for the continuous simulation. The model did not reach “normal” conditions until after approximately 2 simulated years, reflected in the statistical comparisons for 2007 and 2008, which were considerably lower than the following 5 years (2009–2014). Statistical comparisons during a 5-year period (2009–2014) were made using 6 statistical parameters to assess the accuracy of ICPR model stage to observed stage information (Appendix D).

5. Results and discussion

5.1. Peak inflow reduction (historical period)

Greater peak inflow reduction was achieved for LID Scenario 2 (all locations, Tables 5 and 6) because LID Scenario 2 corresponds

Table 5
Peak inflow reduction for historical frontal storm event (February 3rd, 2006) + SLR.

NA4669		NA4670		NC3642		NB4500		NC3230	
LID Scenario 1	LID Scenario 2								
5.17%	9.69%	5.39%	10.62%	0.579%	1.161%	1.309%	2.402%	-0.095%	-0.175%

Table 6
Peak inflow reduction for historical convective storm event (June 24th, 2012) + SLR.

NA4669		NA4670		NC3642		NB4500		NC3230	
LID Scenario 1	LID Scenario 2								
2.65%	5.56%	4.17%	10.00%	0.32%	0.61%	1.15%	2.54%	-0.10%	-0.17%

Table 7
Peak inflow reduction for future May 2030 frontal storm (frontal rainfall pattern #1 + SLR).

NA4669		NA4670		NC3642		NB4500		NC3230	
LID Scenario 1	LID Scenario 2								
5.17%	9.69%	5.39%	10.62%	0.579%	1.161%	1.309%	2.402%	-0.095%	-0.175%

Table 8
Peak inflow reduction for future October 2030 convective storm (convective rainfall pattern #1 + SLR).

NA4669		NA4670		NC3642		NB4500		NC3230	
LID Scenario 1	LID Scenario 2								
2.65%	5.56%	4.17%	10.00%	0.32%	0.61%	1.15%	2.54%	-0.10%	-0.17%

Table 9
Peak inflow reduction for future May 2030 frontal storm (frontal rainfall pattern #2 + SLR).

NA4669		NA4670		NC3642		NB4500		NC3230	
LID Scenario 1	LID Scenario 2								
3.4%	6.9%	2.60%	5.23%	0.371%	0.736%	0.590%	1.207%	-0.070%	-0.118%

Table 10
Peak inflow reduction for future October 2030 convective storm (convective rainfall pattern #2 + SLR).

NA4669		NA4670		NC3642		NB4500		NC3230	
LID Scenario 1	LID Scenario 2								
9.02%	12.5%	11.6%	13.5%	-0.71%	-0.45%	-1.76%	-0.36%	-2.119%	-2.218%

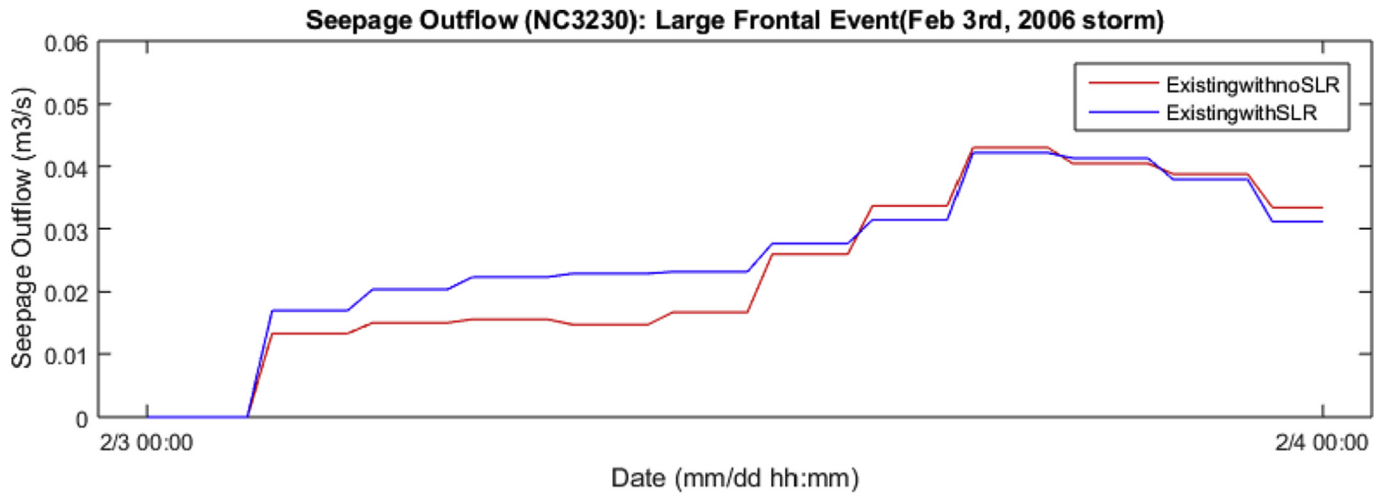


Fig. 19. Seepage Outflow into Cross Bayou Canal at node location NC3230 under existing infrastructure conditions with no SLR and with SLR.

with decreased imperviousness. With respect to NC3230, an increase in peak inflow occurred for both LID Scenario 1 and LID Scenario 2 (denoted by a negative sign), possibly due to rising groundwater tables at that specific location (within the Cross Bayou Canal), with LID Scenario 2 having the greatest increase in peak inflow compared to LID Scenario 1 for both storm types. Peak inflow reduction was much lower for NB4500 than expected, indicating other factors possibly at the subsurface.

5.2. Peak inflow reduction (future period-2030)

Results of peak inflow reduction for future frontal and convective storms (Tables 7 and 8) are similar to the historical frontal and convective storms (Tables 5 and 6) because of the similar defined rainfall patterns. LID Scenario 2 provides the greatest peak inflow reduction, as expected, except for location NC3230 where LID Scenario 2 causes the greatest increase in peak inflow compared to LID Scenario 1 (Table 9). The greatest peak inflow reduction occurred at Nodes NA4669 and NA4670 in Table 10. However, the greatest increase in peak inflow occurs at locations downstream (NC3642, NB4500, NC3230) of upstream locations (NA4669 and

NA4670) (Table 10). Considering the storms defined in Tables 7 and 9 fall under the same storm magnitude, they are associated with a different frontal rainfall pattern which results in the variation in peak inflow reduction values between them. Similarly, for storms defined in Tables 8 and 10, which have the same storm magnitude, their convective rainfall patterns are different resulting in differences in peak inflow reduction. This indicates that rainfall patterns are important in this analysis.

5.3. Groundwater impacts & sea level rise

A separate analysis was completed to determine how (1) the impacts sea level rise and (2) increased perviousness upstream via LID implementation under sea level rise could change groundwater flow along the Cross Bayou tide canal. Nodes NC3642 and NC3230 represent locations within the Cross Bayou canal where seepage outflow information can be obtained. For both node locations, seepage outflow information was obtained for four simulations for both the large convective (June 24, 2012, rainfall pattern) and frontal (February 3, 2006, rainfall pattern) events: (1) existing land use/infrastructure with no sea level rise, (2) existing land-use/

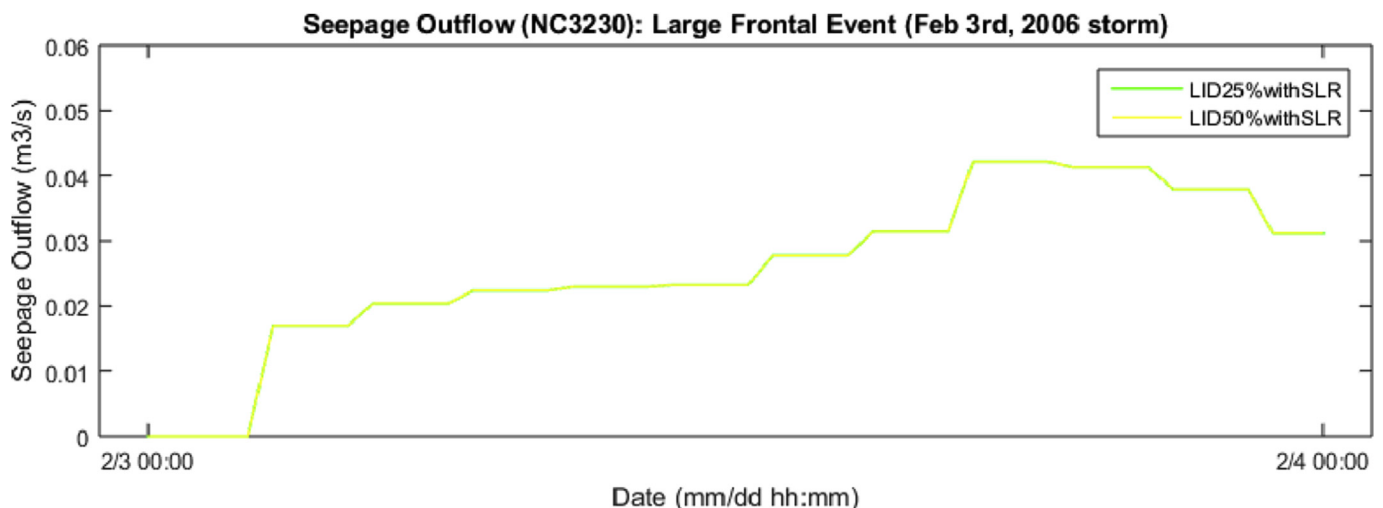


Fig. 20. Seepage Outflow into Cross Bayou Canal at node location NC3230 under LID Scenario 1 (25% impervious reduction) with SLR and NC3230 under LID Scenario 2 (50% impervious reduction) with SLR.

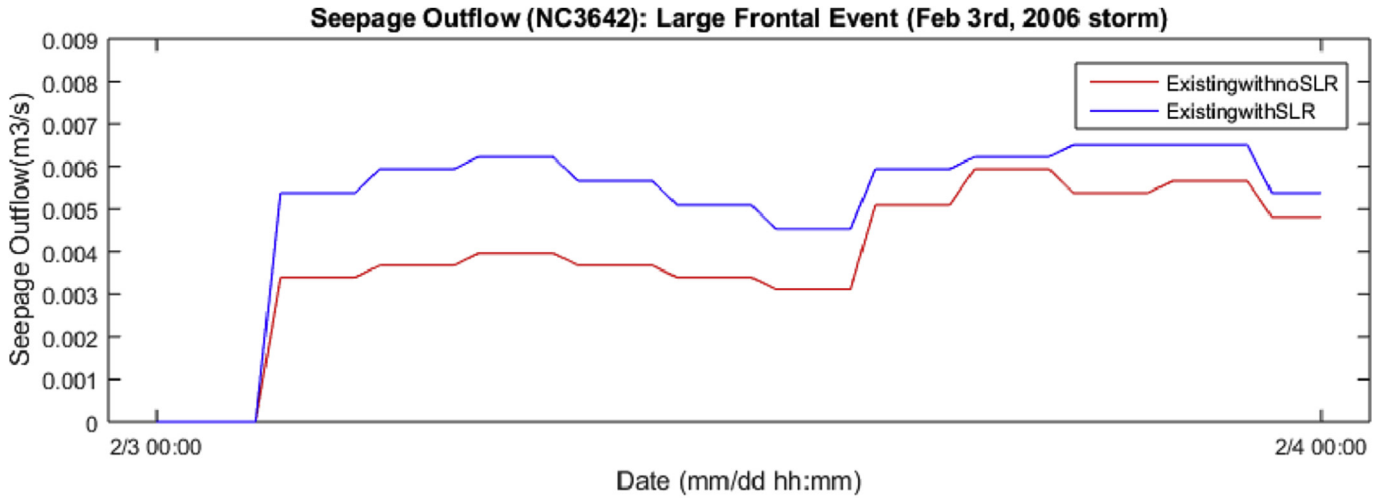


Fig. 21. Seepage Outflow into Cross Bayou Canal at node location NC3642 under existing infrastructure conditions with no SLR and with SLR.

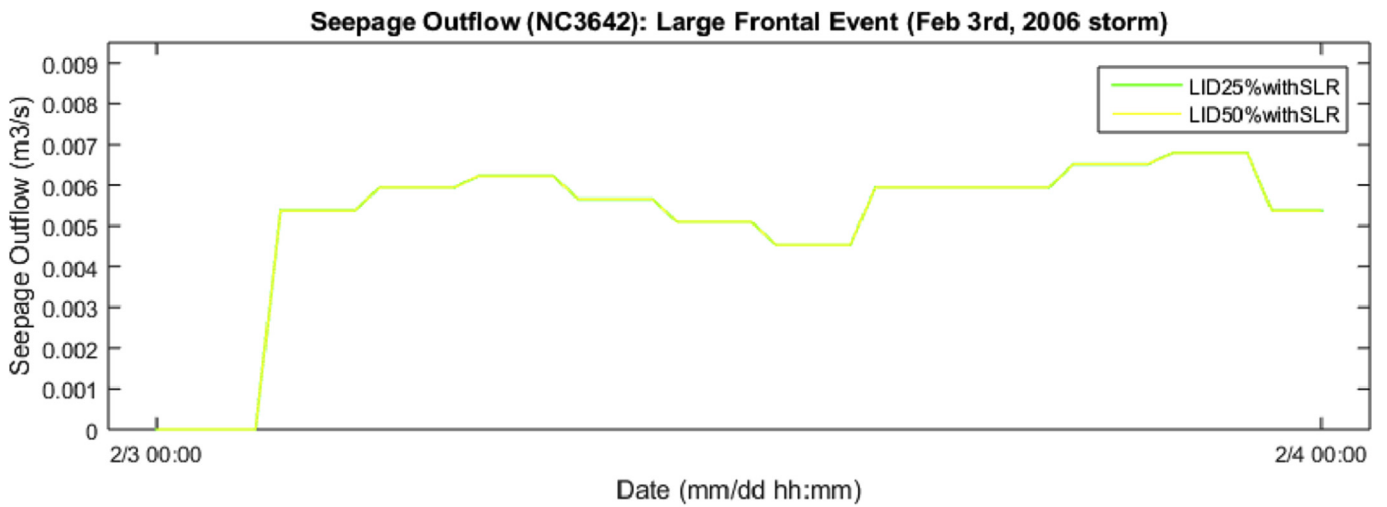


Fig. 22. Seepage Outflow into Cross Bayou Canal at node location NC3642 under LID Scenario 1 (25% impervious reduction) with SLR and NC3642 under LID Scenario 2 (50% impervious reduction) with SLR.

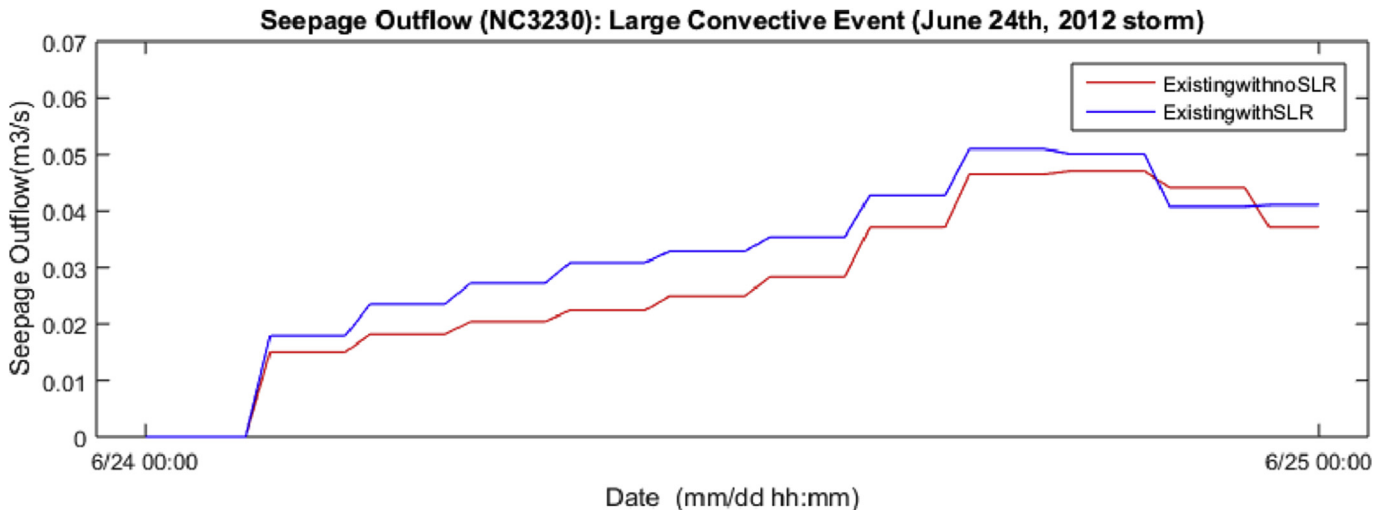


Fig. 23. Seepage Outflow into Cross Bayou Canal at node location NC3230 under existing infrastructure conditions with no SLR and with SLR.

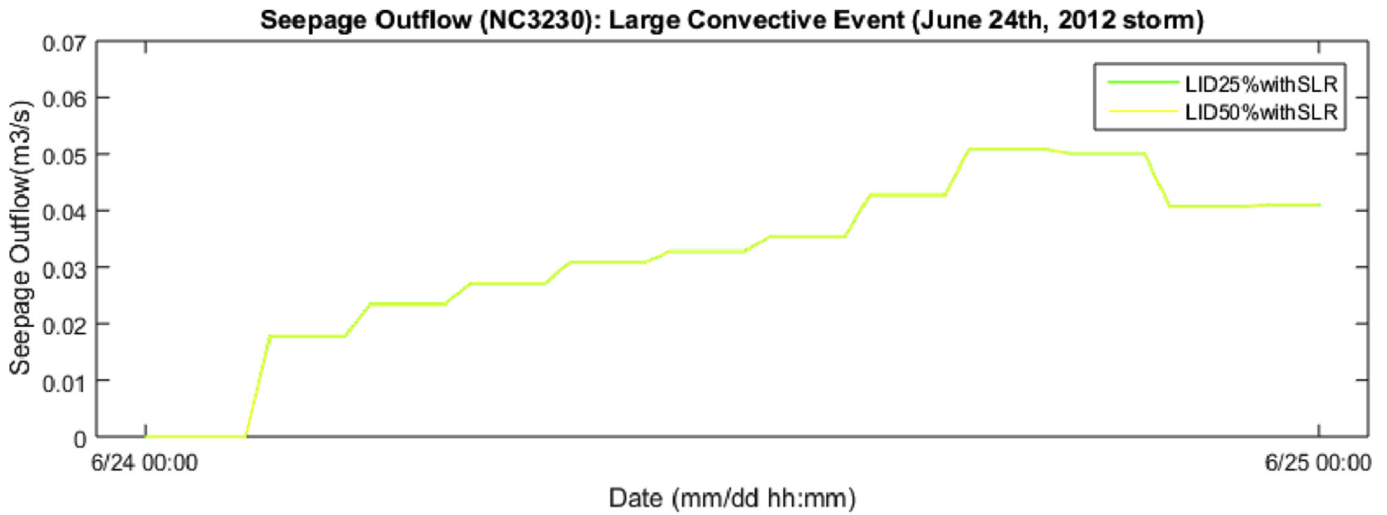


Fig. 24. Seepage Outflow into Cross Bayou Canal at node location NC3230 under LID Scenario 1 (25% impervious reduction) with SLR and NC3230 under LID Scenario 2 (50% impervious reduction) with SLR.

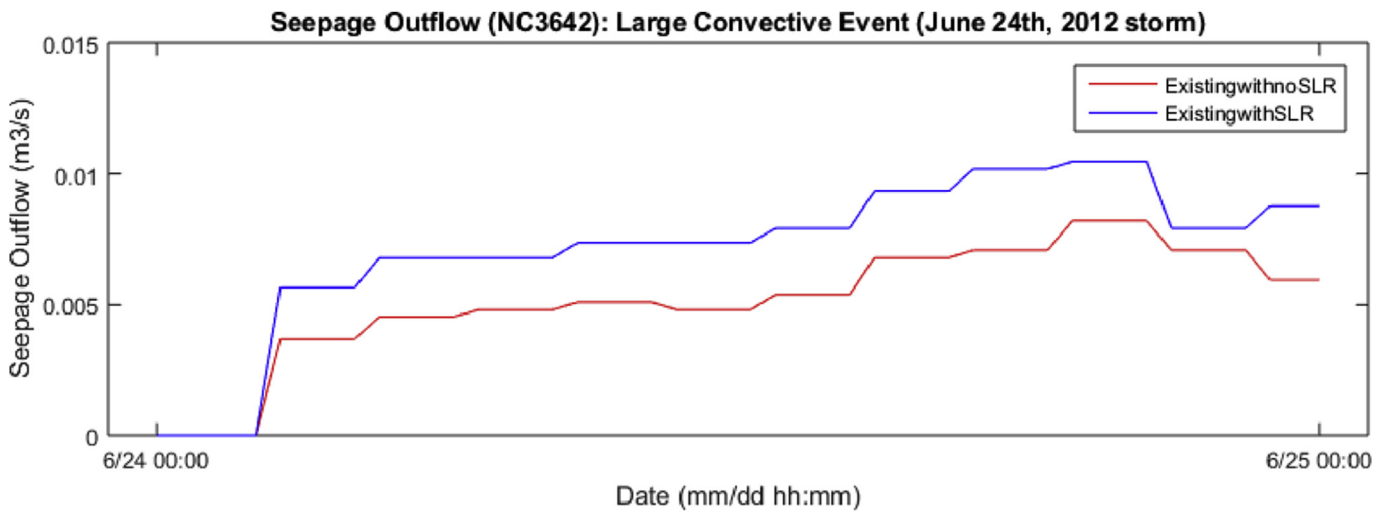


Fig. 25. Seepage Outflow into Cross Bayou Canal at node location NC3642 under existing infrastructure conditions with no SLR and with SLR.

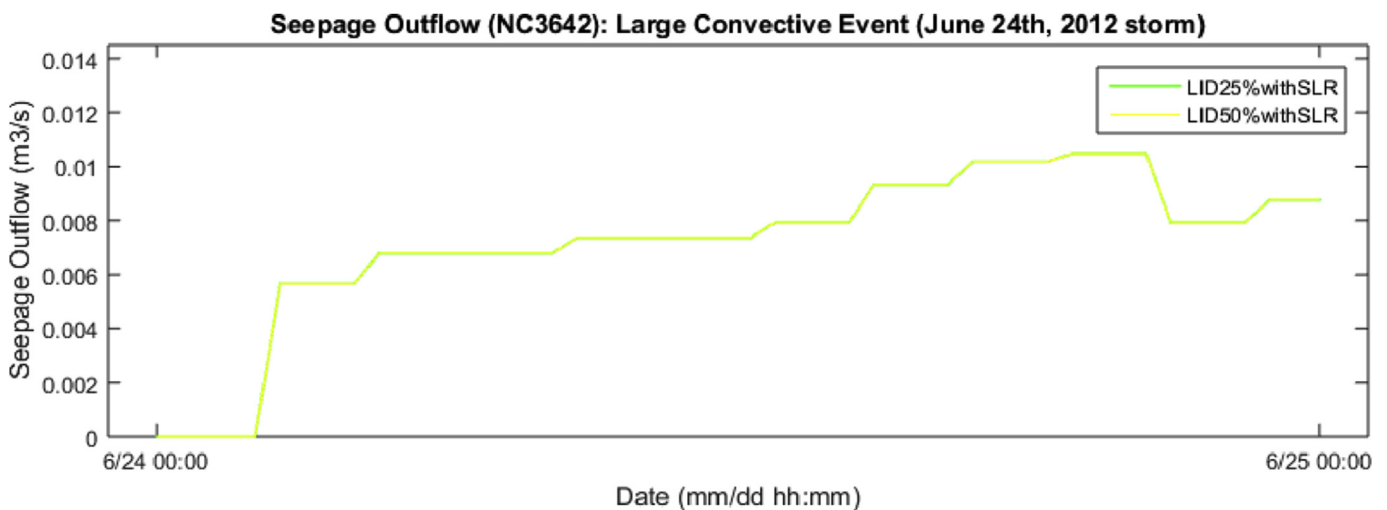


Fig. 26. Seepage Outflow into Cross Bayou Canal at node location NC3230 under LID Scenario 1 (25% impervious reduction) with SLR and NC3230 under LID Scenario 2 (50% impervious reduction) with SLR.

infrastructure with sea level rise, (3) 25% impervious reduction (Scenario 1) with sea level rise, and (3) 50% impervious reduction (Scenario 2) with sea level rise.

Without LID implementation (Figs. 19, 21, 23 and 25), greater seepage outflow from the groundwater table into the Cross Bayou canal occurs under SLR as opposed to without SLR. Considering LID implementation only (Figs. 20, 22, 24 and 26), seepage outflow from the groundwater table remained constant between LID scenarios. Overall the seepage outflow rates from the groundwater table were considerably lower for the frontal event (Figs. 19, 20, 21 and 22) as opposed to seepage outflow rates during the convective event (Figs. 23, 24, 25 and 26).

Seepage outflow from the groundwater table into the Cross Bayou Canal are reflected in peak inflow reduction trends at node locations within the Cross Bayou Canal. For instance, at nodes NC3230 and NC3642, lower seepage outflow for the frontal event (Figs. 20 and 22) resulted in greater peak inflow reduction (Table 5), whereas a higher seepage outflow for the convective event resulted in lower peak inflow reduction at nodes NC3230 and NC3642 (Table 6).

6. Conclusion

As reflected in this study, rainfall type affects LID implementation strategies when considering rainfall runoff reduction via the peak inflow reduction metric. Variations in sub-daily rainfall patterns also affects rainfall runoff reduction regardless of whether total daily rainfall is the same. Sea level rise effects on the groundwater table also affects the ability to incorporate infiltration-based LID alternatives to reduce imperviousness. Adding infiltration-based LID alternatives to areas affected by sea level

rise could result in higher groundwater tables for these areas. For these reasons, before LID implementation can be evaluated as an adaptive stormwater drainage measure, rainfall type, sub-daily rainfall patterns, and a groundwater analysis must be considered under chosen “design-storm” magnitude(s). Overall LID implementation within a watershed can alter the hydrologic response of existing grey drainage infrastructure as to offer increased peak inflow reduction across varying rainfall type and sub-daily rainfall patterns. The deployment of LID to capture runoff under various storm scenarios associated with rainfall types and patterns while accounting for subsurface processes would be beneficial when considering long-term drainage resilience.

Acknowledgements

The authors are grateful for the financial support via the Florida Sea Grant College Program, a partnership between the Florida Board of Education, the National Oceanic and Atmospheric Administration, and Florida’s citizens and governments, under project R-CS-58 with assistance from the Pinellas County Government. Southwest Florida Water Management District for making available sub-daily rainfall data. The authors are thankful for the constructive and copious comments received from anonymous reviewers who helped improve the quality of the paper.

Appendix A. LID technology hub

Table A.1
Summary of point-based LID technologies

Low Impact Development	Description	Ecosystem Services
<p>Retention basin</p>  <p>http://www.stormwaterpa.org</p>	<ul style="list-style-type: none"> ■ A recessed area within the landscape that is designed to store and retain a defined quantity of runoff, allowing it to percolate through permeable soils into the groundwater. 	<ul style="list-style-type: none"> ■ Reduces stormwater volume, which reduces the average annual pollutant loading that may be discharged from the system. ■ Suspended solids, heavy metals, bacteria, pesticides, and nutrients are removed as runoff percolates through the soil profile.
<p>Treatment swales</p>  <p>http://www.dot.ca.gov</p>	<ul style="list-style-type: none"> ■ Have been used for conveyance of stormwater along roads for decades. ■ When properly designed and maintained, swales can be used for stormwater treatment, providing retention and infiltration of stormwater. 	<ul style="list-style-type: none"> ■ Provides reduction of stormwater volume which reduces pollutant loads. ■ Suspended solids, oxygen demanding materials, heavy metals, bacteria, some varieties of pesticides, and nutrients may be removed as runoff percolates through the soil profile.

(continued on next page)

Table A.1 (continued)

Low Impact Development	Description	Ecosystem Services
<p>Pervious pavement</p>  <p>http://nacto.org Greenroof/Cistern</p>  <p>http://greencitygrowers.com</p>	<ul style="list-style-type: none"> ■ Pervious pavement systems include the subsoil, the sub-base, and the pervious pavement and include several types of designed systems such as pervious concrete, pervious aggregate products, pervious paver systems, and modular paver systems. ■ A vegetated roof followed by filtrate storage in a cistern, which can be reused. ■ The filtrate from the greenroof is collected in a cistern or, if the greenroof is part of a BMP treatment train, the filtrate may be discharged to a downstream BMP. 	<ul style="list-style-type: none"> ■ Pervious pavement systems are retention systems and should be used as part of a treatment train to reduce stormwater volume and pollutant load from parking lots, or similar types of areas. ■ The greenroof/cistern system functions to attenuate, evaporate, and lower the volume of discharge and pollutant load coming from the roof surface. ■ Greenroof systems have been shown to assist in stormwater management by attenuating hydrographs, neutralizing acid rain, reducing volume of discharge, and reducing the annual mass of pollutants discharged.

Source: Pinellas County Stormwater Manual, 2015

Appendix B. SDSM calibration and validation

Table B.1
Predictor variables used for future rainfall projection

Center/agency & climate scenario	Variable	Variable description
Hadley Center CM4 AR4 A2	h3a2p_fna	Surface airflow strength
	h3a2p_una	Surface zonal velocity
	h3a2p_vna	Surface meridional velocity
	h3a2p_zna	Surface vorticity
	h3a2p_zhna	Surface divergence
	h3a2p5_fna	500 hPa airflow strength
	h3a2p5_una	500 hPa zonal velocity
	h3a2p5_vna	500 hPa meridional velocity
	h3a2p5_zna	500 hPa vorticity
	h3a2p500na	500 hPa geopotential height
	h3a2p5zhna	500 hPa Surface divergence
	h3a2shumna	Surface specific humidity

Table B.2
SDSM Monthly Calibration Statistics

Month	R-Squared
January	0.329
February	0.477
March	0.266
April	0.559
May	0.429
June	0.076
July	0.136
August	0.176
September	0.117
October	0.840
November	0.400
December	0.217

Note: Monthly SDSM calibration for Period of Sept 1998-Sept 2010 using log-transform of daily rainfall record for the same period and HADCM3 AR4 A2 predictor variables. R-squared represents goodness of fit of predictor variables in explaining occurrence of rainfall on a monthly basis for each station.

Observed vs. SDSM Monthly Mean Rainfall (Jan 2011-Jan 2014)

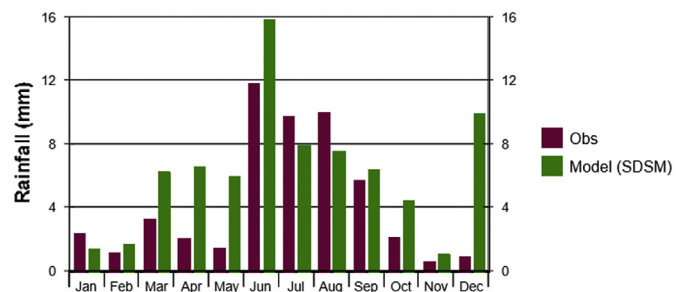


Fig. B.1. Observed vs. SDSM mean monthly rainfall for validation period (Jan 2011–2014).

Observed vs. SDSM Monthly Variance (Jan 2011-2014)

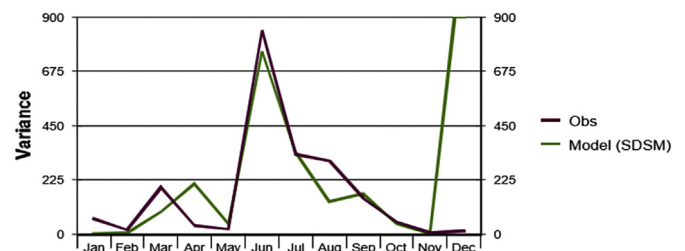


Fig. B.2. Observed vs. SDSM monthly variance for validation period (Jan 2011–2014).

Appendix C. Green-Ampt parameters based upon NRCS soil zone survey

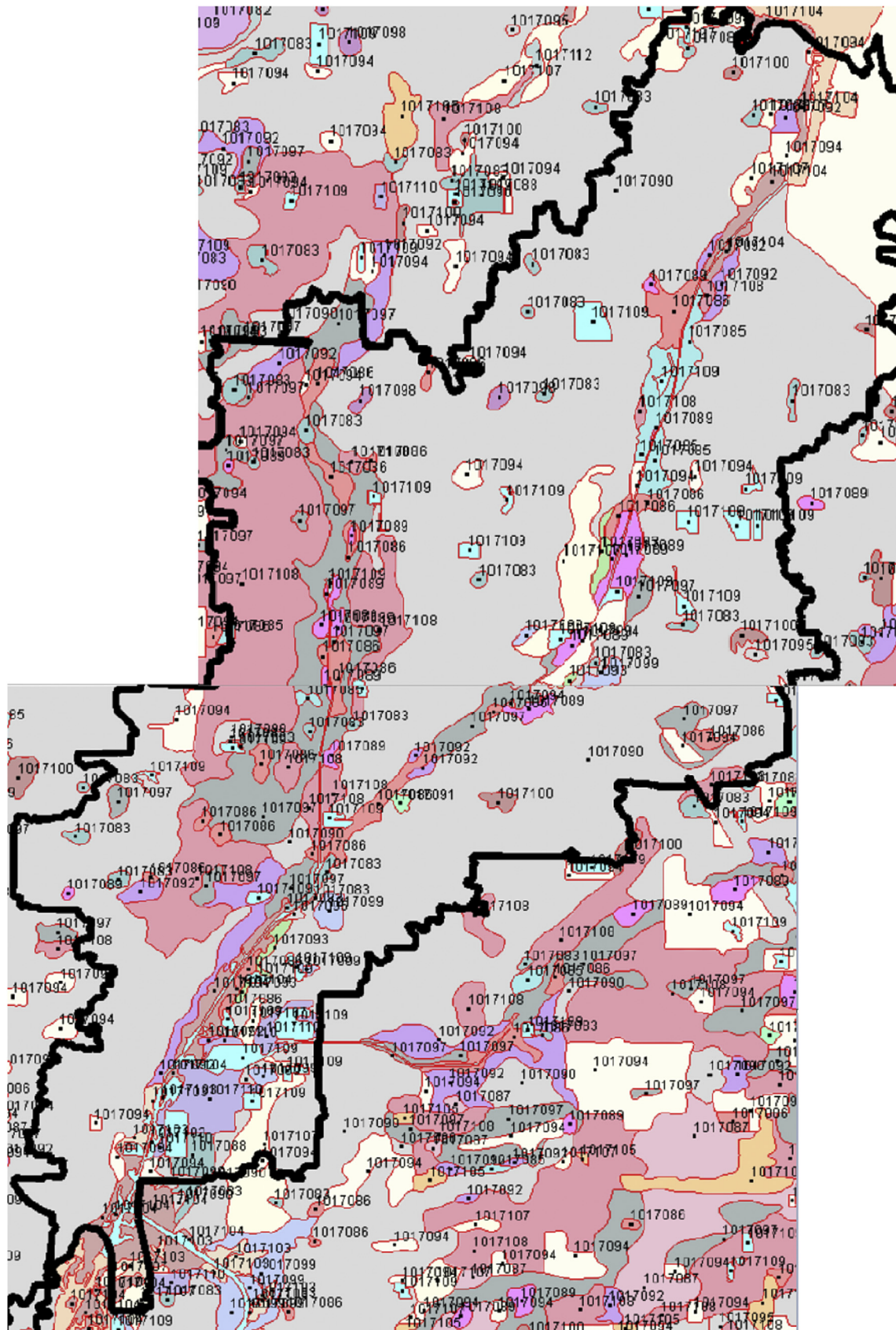


Fig. C.1. NRCS Soil Zone Classification.

Table C.1

Original Green-Ampt Parameters based upon NRCS analysis

Soil Zone	Vertical Hydraulic Cond. (m/d)	Saturated Moisture Content	Residual Moisture Content	Initial Moisture Content	Field Moisture Content	Wilting Moisture Content	Pore Size Index	Bubble Pressure (cm)	Allow Recharge	Initial Water Table(m)
1017080	7.895	0.411	0.003	0.020	0.020	0.005	0.568	4.144	Yes	0.790
1017083	7.930	0.440	0.033	0.145	0.145	0.065	0.496	2.499	Yes	0.010
1017106	20.128	0.401	0.002	0.013	0.013	0.004	0.570	4.327	Yes	1.080
1017100	7.951	0.399	0.007	0.036	0.036	0.013	0.561	4.162	Yes	0.080
1017112	7.817	0.422	0.016	0.093	0.093	0.031	0.560	3.673	Yes	0.030
1017088	11.940	0.394	0.002	0.012	0.012	0.004	0.570	4.440	Yes	0.310
1017092	4.552	0.412	0.011	0.053	0.053	0.021	0.495	3.870	Yes	0.360
1017087	7.276	0.407	0.010	0.050	0.050	0.019	0.481	4.004	Yes	0.140
1017086	7.133	0.417	0.017	0.087	0.087	0.033	0.488	3.797	Yes	0.180
1017107	6.897	0.408	0.007	0.042	0.042	0.014	0.553	3.849	Yes	0.360
1017104	6.926	0.443	0.030	0.123	0.123	0.059	0.521	3.834	Yes	0.010
1017089	1.779	0.422	0.023	0.103	0.103	0.045	0.471	3.610	Yes	0.050
1017094	6.262	0.424	0.014	0.068	0.068	0.028	0.515	3.652	Yes	0.690
1017090	6.977	0.402	0.008	0.045	0.045	0.015	0.575	4.430	Yes	0.360
1017091	7.951	0.828	0.007	0.745	0.745	0.429	0.392	22.617	Yes	0.080
1017096	20.558	0.403	0.008	0.038	0.038	0.016	0.581	4.590	Yes	1.450
1017085	5.087	0.407	0.012	0.050	0.050	0.023	0.488	4.046	Yes	0.140
1017097	6.409	0.422	0.015	0.062	0.062	0.029	0.493	3.227	Yes	0.290
1017110	6.483	0.395	0.001	0.004	0.004	0.002	0.541	4.311	Yes	0.380
1017098	7.879	0.453	0.013	0.080	0.080	0.025	0.516	2.651	Yes	0.160
1017099	6.927	0.411	0.004	0.030	0.030	0.008	0.573	4.264	Yes	0.790
1017095	7.951	0.732	0.028	0.416	0.416	0.201	0.396	5.218	Yes	0.020
1017093	7.913	0.419	0.008	0.045	0.045	0.016	0.532	3.296	Yes	0.720
1017082	7.911	0.398	0.003	0.023	0.023	0.006	0.572	4.422	Yes	1.400
1017105	6.262	0.424	0.014	0.068	0.068	0.028	0.515	3.652	Yes	2.011
1017108	5.873	0.398	0.011	0.055	0.055	0.022	0.493	4.150	Yes	0.360
1017103	7.723	0.667	0.025	0.371	0.371	0.180	0.418	5.473	Yes	0.020
1017109	6.262	0.424	0.014	0.068	0.068	0.028	0.515	3.652	Yes	0.003
1017111	6.262	0.424	0.014	0.068	0.068	0.028	0.515	3.652	Yes	0.003
OFFSITE	6.262	0.424	0.014	0.068	0.068	0.028	0.515	3.652	No	0.610

Table C.2

Calibrated Green-Ampt Parameters for ICPR Model

Soil Zone	Vertical Hydraulic Cond. (m/d)	Saturated Moisture Content	Residual Moisture Content	Initial Moisture Content	Field Moisture Content	Wilting Moisture Content	Pore Size Index	Bubble Pressure (cm)	Allow Recharge	Initial Water Table(m)
1017080	0.305	0.400	0.003	0.250	0.250	0.125	0.568	4.144	Yes	0.790
1017083	0.305	0.400	0.033	0.250	0.250	0.125	0.496	2.499	Yes	1.080
1017106	0.305	0.400	0.002	0.250	0.250	0.125	0.570	4.327	Yes	0.720
1017100	0.305	0.400	0.007	0.250	0.250	0.125	0.561	4.162	Yes	0.380
1017112	0.305	0.400	0.016	0.250	0.250	0.125	0.566	3.371	Yes	0.000
1017088	0.305	0.400	0.002	0.250	0.250	0.125	0.569	4.601	Yes	0.360
1017092	0.305	0.400	0.011	0.250	0.250	0.125	0.494	3.969	Yes	0.010
1017087	0.305	0.400	0.010	0.250	0.250	0.125	0.480	4.131	Yes	0.310
1017086	0.305	0.400	0.017	0.250	0.250	0.125	0.487	4.037	Yes	0.010
1017107	0.305	0.400	0.007	0.250	0.250	0.125	0.553	3.849	Yes	1.400
1017104	0.305	0.400	0.030	0.250	0.250	0.125	0.531	3.181	Yes	0.790
1017089	0.305	0.400	0.023	0.250	0.250	0.125	0.470	3.746	Yes	0.080
1017094	0.305	0.400	0.014	0.250	0.250	0.125	0.520	3.198	Yes	0.690
1017090	0.305	0.400	0.008	0.250	0.250	0.125	0.575	4.430	Yes	0.060
1017091	0.305	0.400	0.007	0.250	0.250	0.125	0.405	4.572	Yes	0.360
1017096	0.305	0.400	0.008	0.250	0.250	0.125	0.581	4.590	Yes	0.010
1017085	0.305	0.400	0.012	0.250	0.250	0.125	0.486	4.347	Yes	0.080
1017097	0.305	0.400	0.015	0.250	0.250	0.125	0.493	3.261	Yes	1.450
1017110	0.305	0.400	0.001	0.250	0.250	0.125	0.543	4.053	Yes	0.020
1017098	0.305	0.400	0.013	0.250	0.250	0.125	0.516	2.651	Yes	0.010
1017099	0.305	0.400	0.004	0.250	0.250	0.125	0.573	4.264	Yes	0.290
1017095	0.305	0.400	0.027	0.250	0.250	0.125	0.385	6.043	Yes	0.360
1017093	0.305	0.400	0.008	0.250	0.250	0.125	0.532	3.296	Yes	0.020
1017082	0.305	0.400	0.003	0.250	0.250	0.125	0.572	4.422	Yes	0.010
1017105	0.305	0.400	0.008	0.250	0.250	0.125	0.575	4.430	Yes	0.020
1017108	0.305	0.400	0.011	0.250	0.250	0.125	0.492	4.258	Yes	0.360
1017103	0.305	0.400	0.023	0.250	0.250	0.125	0.397	7.212	Yes	0.030
1017109	0.305	0.400	0.003	0.250	0.250	0.125	0.568	4.144	Yes	0.360
1017111	0.305	0.400	0.003	0.250	0.250	0.125	0.568	4.144	Yes	0.000
OFFSITE	0.305	0.400	0.014	0.250	0.250	0.125	0.515	3.652	No	0.610

Note: During the initial simulations of a June 21–30, 2012 storm event for ICPR calibration, infiltration and recharge to the groundwater appeared high for pervious areas based on comparison with observed data. This resulted in lower modeled stages than observed at both of the USGS gauges. Low runoff volumes were caused by high saturated vertical conductivities based on the weighted average Green-Ampt parameters. It is believed that compaction in urban areas and “thatching” of grassed areas likely reduces the vertical conductivity at the surface. Thatching is caused by the build-up of organic matter (grass clippings) at the surface of the soils and can significantly reduce infiltration rates (Streamline Technologies, Inc., 2015) For this reason, calibrated vertical hydraulic conductivity values (Column 2) appear to be much lower and uniform than recorded by NRCS.

Appendix D. ICPR validation results

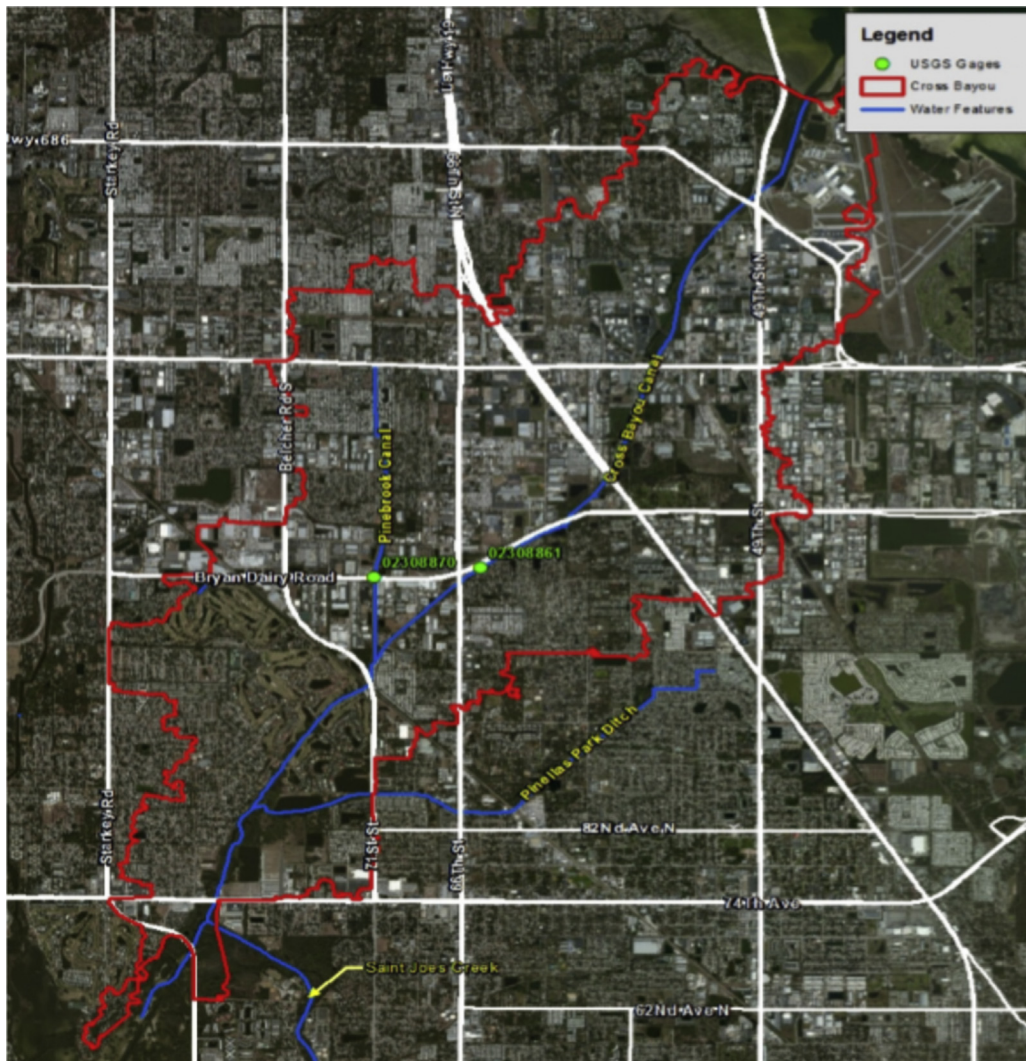


Fig. D.1. Location of USGS gauge stations for ICPR model validation (Source: Streamline Technologies, Inc., 2015).

Table D.1

USGS Gauge 02308861 Statistical Metrics

Period of Record	# of Gauge Measurements	R	R ²	ME	MAE	RMSE	N-S
01/01/2007- 01/01/2014	121,954	0.841	0.708	0.101	0.224	0.305	0.624
01/01/2009- 01/01/2014	86,872	0.865	0.748	0.065	0.208	0.283	0.705

Note: Gauge measurements are for stage. Six statistical metrics were considered: Correlation Coefficient (R), Coefficient of Determination (R²), Mean Error (ME), Mean Absolute Error (MAE), Root Mean Square Error (RMSE) and Nash-Sutcliffe Model Efficiency Coefficient (N-S). The statistical metrics are unitless and can be multiplied by 100 to obtain percentages.

Table D.2

USGS Gauge 02308860 Statistical Metrics

Period of Record	# of Gauge Measurements	R	R ²	ME	MAE	RMSE	N-S
01/01/2007- 01/01/2014	122,606	0.895	0.807	0.014	0.049	0.092	0.794
01/01/2009- 01/01/2014	87,539	0.910	0.827	0.025	0.050	0.096	0.815

Note: Gauge measurements are for stage. Six statistical metrics were considered: Correlation Coefficient (R), Coefficient of Determination (R²), Mean Error (ME), Mean Absolute Error (MAE), Root Mean Square Error (RMSE) and Nash-Sutcliffe Model Efficiency Coefficient (N-S). The statistical metrics are unitless and can be multiplied by 100 to obtain percentages.

References

- Abbott, M., 1991. *Hydroinformatics: Information Technology and the Aquatic Environment*. Avebury Technical Brookfield, USA.
- Ali, A., Abtew, W., Van Horn, S., Khanal, N., 2000. Temporal and spatial characterization of rainfall over Central and South Florida. *J. Am. Water Resour. Assoc.* 36, 833–848.
- Birgani, Y.T., Yazdandoost, F., Moghadam, M., 2013. Role of resilience in sustainable urban stormwater management. *Hydraul. Struct.* 1 (1), 44–53.
- Clar, M., Barfield, B.J., O'Conner, T., 2004. *Stormwater Best Management Practices Design Guid Volume 1-General Considerations*. U.S. Environmental Protection Agency, Washington, DC. EPA/600/R-04/121.
- De Bruijn, K.M., 2004. Resilience and flood risk management. *Water Policy* 6, 53–66.
- Federal Highway Administration (FHWA), 1984. HEC 19-Hydrology. Accessed October 2016. Available online at: http://www.fhwa.dot.gov/engineering/hydraulics/library_listing.cfm?archived=true.
- Florida Department of Environmental Protection, 2014. Chapter 62-25 Regulations of Stormwater Discharge. Accessed October 2016. Available online at: <http://www.dep.state.fl.us/legal/Rules/surfacewater/62-25.pdf>.
- Hernandez, Tatiana X., 2001. *Rainfall-runoff modeling in humid shallow water table environments*. Graduate Theses and Dissertations. Accessed October 2016. Available online at: <http://scholarcommons.usf.edu/etd/1537>.
- Holling, C.S., 1973. Resilience and stability of ecological systems. *Annu. Rev. Ecol. Syst.* 1–23.
- Hosking, J.R.M., Wallis, J.R., 1997. *Regional Frequency Analysis, An Approach Based on L-moments*. Cambridge University Press.
- Huff, F.A., 1967. Time distribution of rainfall in heavy storms. *Water Resour. Res.* 3 (4), 1007–1019.
- Huff, F.A., 1990. Time distributions of heavy rainstorms in Illinois: Champaign, Illinois. *Illinois State Water Survey*, p. 173. Circular.
- IPCC, 2014. Summary for policymakers. In: Field, C.B., Barros, V.R., Dokken, D.J., Mach, K.J., Mastrandrea, M.D., Bilir, T.E., Chatterjee, M., Ebi, K.L., Estrada, Y.O., Genova, R.C., Girma, B., Kissel, E.S., Levy, A.N., MacCracken, S., Mastrandrea, P.R., White, L.L. (Eds.), *Climate Change 2014: Impacts, Adaptation, and Vulnerability. Part A: Global and Sectoral Aspects. Contribution of Working Group II to the Fifth Assessment Report of the Intergovernmental Panel on Climate Change*. Cambridge University Press, Cambridge, United Kingdom and New York, NY, USA, pp. 1–32.
- Jones Edmunds and Associates, Inc., 2013. *Floodplain Analysis, Cross Bayou Watershed Management Plan*. Pinellas County Board of County Commissioners and Southwest Florida Water Management District.
- Koutsyiannis, D., Onof, C., Wheeler, H.S., 2003. Multivariate rainfall disaggregation at a fine timescale. *Water Resour. Res.* 39, 1173.
- Laniak, G.F., Olchin, G., Goodall, J., Voinov, A., Hill, M., Glynn, P., Whelan, G., Geller, G., Quinn, N., Blind, M., Peckham, S., Reaney, S., Gaber, N., Kennedy, R., Hughes, A., 2013. Integrated environmental modeling: a vision and roadmap for the future. *Environ. Model. Softw.* 39, 3–23.
- Natural Resources Conservation Service (NRCS), 1986. *Urban Hydrology for Small Watersheds, Technical Release 55*. USDA.
- NOAA, 2013. *Precipitation-frequency Atlas of the United States, Southeastern States (Alabama, Arkansas, Florida, Georgia, Louisiana, Mississippi)*. Accessed September 2016. [Available online at: http://www.nws.noaa.gov/oh/hdsc/PF_documents/Atlas14_Volume9.pdf].
- NOAA, 2016a. *Sea Level Trends*. Accessed August 2016. Available online at: <https://tidesandcurrents.noaa.gov/sltrends/sltrends.html>.
- NOAA, 2016b. *The Coastal Population Explosion*. Available online at: http://oceanservice.noaa.gov/websites/retiredsites/natdia_pdf/3hinrichsen.pdf.
- Omer, M., 2013. *The resilience of networked infrastructure systems*. World Scientific.
- Pinellas County Planning Department, 2015. *Pinellas County Stormwater Manual Jan 2015*. Available online at: <http://www.pinellascounty.org>.
- Pinellas County Planning Department, 2016. *Pinellas County Stormwater Manual May 2016*. Available online at: <http://www.pinellascounty.org>.
- Price, R.K., Vojinovic, Z., 2008. Urban flood disaster management. *Urban Water J.* 5 (3), 259–276. <http://dx.doi.org/10.1080/15730620802099721>.
- Pui, A., Sharma, A., Mehrotra, R., Sivakumar, B., Jeremiah, E., 2012. A comparison of alternatives for daily to sub-daily rainfall disaggregation. *J. Hydrol.* 138, 470–471.
- Qin, H-p., Li, Z-x., Fu, G., 2013. The effects of low impact development on urban flooding under different rainfall characteristics. *J. Environ. Manag.* 129 (15), 577–585.
- Roseen, R., T. Janeski, M. Simpson, J. Houle, J. Gunderson, & T. Ballestero. 2012: *Economic and Adaptation Benefits of Low Impact Development*. Conference Proceedings, 2011 Low Impact Development Symposium. Accessed Feb 2016. Available online at: www.unh.edu/unhsc/sites/unh.edu/unhsc/files/pubs_specs_info/JEE%20FTL%203-30-12.b.pdf.
- Soil Conservation Service, 1973. *A method for estimating volume and rate of runoff in small watersheds*. U.S. Department of Agriculture, Soil Conservation Service, Washington, D.C. SCS-TP-149.
- Southwest Florida Water Management District (SWFWMD), 2013. *Environmental Resource Permit Applicant's Handbook Volume II-design Requirements for Stormwater Treatment and Management Systems Water Quality and Water Quantity*. Accessed October 2016. Available online at: https://www.swfwmd.state.fl.us/files/database/site_file_sets/2479/Applicants_Handbook_II_-_Revised.pdf.
- Streamline Technologies, Inc., 2015. *An Integrated Surface Water-groundwater Model of the Cross Bayou Watershed*.
- Tampa Bay Climate Science Advisory Panel, 2015. *Recommended Projection of Sea Level Rise in the Tampa Bay Region*. Available online at: http://www.tbrc.org/council_members/councilagendas/2015/101215/8c.pdf.
- UN-Habitat, 2012. *State of the World's Cities 2012/2013, Prosperity of Cities State of the World's Cities, State of the World's Cities*. UN-Habitat.
- Wey, K., 2007. *Temporal Disaggregation of Daily Precipitation Data in a Changing Climate*. UWSpace. <http://hdl.handle.net/10012/2859>.
- Westra, S., Mehrotra, R., Sharma, A., Srikanthan, R., 2012. Continuous rainfall simulation: 1 A regionalized subdaily disaggregation approach. *Water Resour. Res.* 48, W01535. <http://dx.doi.org/10.1029/2011WR010489>.
- Wilby, R.L., Dawson, C.W., Barrow, E.M., 2002. SDSM—a decision support tool for the assessment of regional climate change impacts. *Environ. Model. Softw.* 17 (2), 145–157.
- Zhang, J., Murch, R.R., Ross, M.A., Ganguly, A.R., Nachabe, M., 2008. Evaluation of statistical rainfall disaggregation methods using rain-gauge information for West-Central Florida. *J. Hydrol. Eng.* 13 (12), 1158–1169.